

Serpentinite from the Yazagyo Dam site and its related to that Foundation Problem, Kalay Township, Sagaing Region, Myanmar

Aung Myo Zaw⁽¹⁾, Thiha⁽²⁾, Kyi Kyi Maw⁽³⁾

⁽¹⁾⁽²⁾⁽³⁾Dagon University, Department of Geology, Myanmar

Email: aungmyozaw009@gmail.com

ABSTRACT: The Yazagyo Dam site is situated at about 3.2 km upstream north of Yazagyo village, Kalay Township, Sagaing Region. During the field investigation, serpentine samples are systematically collected to revise the serpentinization stage and to test for rock strength in laboratory. Three types of textures are observed in thin sections: pseudomorphic, non-pseudomorphic and vein. The relic minerals indicate that the original rock was mainly peridotite. In general, the degree of serpentinization may be regarded as partial to nearly complete. Two zones of serpentinization are delineated on a map for the serpentinite body such as P zone (Partial) and C zone (complete). The engineering properties of serpentine rocks are tested by point load test and uniaxial compressive strength test. Due to the nature of serpentine rock, the real value of RQD and compressive strength cannot be measured in usual way of measuring of other rocks. According to the field investigation of the Dam site area most part of the dam foundation area is located on the weathered serpentine body and landslide debris. About six dolerite intrusions into the serpentine body of the Talone Hill are noted, where seepages occur flowing from the contact of jointed dolerite into serpentinized body. Due to the nature of partial serpentinization, dam abutment should be changed to complete serpentinization zone.

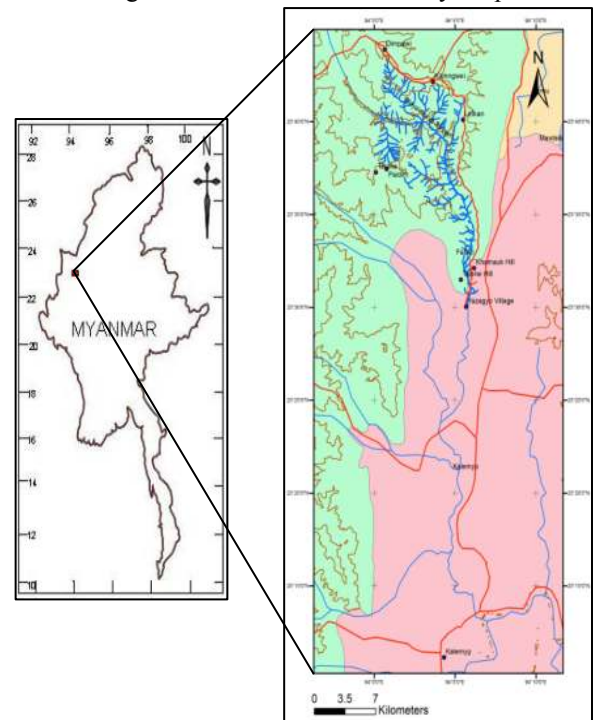
KEYWORDS: *Serpentine texture, zone, engineering properties.*

1. INTRODUCTION

Yazagyo Dam site project is going to be constructed on serpentinite foundation. The area under present research is situated about 3.2 km upstream north of Yazagyo village, Kalay Township, Sagaing Region (Fig.1). The word serpentinized is used as a prefix when amount of serpentine in the rock exceeds 30 percent. If serpentine constitutes more than 95 percent, the rock is termed serpentinite after Coats (1968). Generally it is said that construction of dam on serpentinite is not recommended, because it might have smaller mechanical properties and some failure problems are also recorded in Yazagyo dam site. The noteworthy example of serpentinite foundation problem is saddle (II) failure in (2008). According to Goodman (1993), Dam should not be positioned on serpentinite and that the material is unstable and unsuitable as the foundation for a dam. Taking into account these legitimate published cautions, a through geotechnical investigations should be taken in these serpentine rocks mass. It is currently being constructed

on serpentinite foundation in Myanmar including present dam site and upper Buywa Multipurpose dam site project, Sidoktaya Township after Kyaw Htun et.al (2007). Admitting that the circumstance of serpentinite was bad, they depend on the type of serpentine and serpentinization processes, even though engineering properties of those rocks were diverse. So, this study was carried out to solve the serpentine problem of the Yazagyo Dam site.

Fig 1 Location and Accessibility Map



2. THEORETICAL BACKGROUND

A preliminary survey of the serpentinite samples collection was done by Kyaw Htun et.al in 2009 and they pointed out that the serpentinization processes have not been ceased yet, inspite the occurrence of Mesh texture (serpentine texture) in thin section during the Petrographic studies. After that, during the 2010 Japanese Team of the Sanyu Consultants team were collected the six serpentinite samples for X-ray diffraction analysis to know the serpentinization degree. This team were also suggested that the serpentine of Yazagyo dam site has been well serpentinized and the main mother minerals like olivine and Pyroxene are rarely found in it. In December 2010, the author was able to visit the Yazagyo dam site and serpentinite rock samples are systematically collected for detailed study in laboratory. All of these samples were marked on the

point by using the G.P.S (Global Positioning System) and outcrops nature were comprehensive recorded. The purposes of the collection of samples are (1) to get the data documented for the serpentinization stage of the dam site based on the collected bulk samples, (2) to publicize that the series of landslides are restricted only in serpentinite rock, (3) to know, how to connect nature of water and serpentinite rock in the study area.

3. EXPERIMENT

For the Petrographic study, Petrographic thin sections were made in Department of Geology (Rock cutting room), Dagon University, Myanmar. Another testing, especially rock strength test were made in Department of Mining (Rock Mechanics Laboratory), Yangon Technological University, Myanmar. To know the serpentinization stage detailed Petrographic studies of more than fifty-two thin sections were made. The uniaxial compressive strength test was carried out on four serpentine rock core samples.

3.1 Material and methods

When the first step of sample collection and field observation had been completed, and then collected bulk sample are firstly mesoscopic studies were carried out. The purpose of samples collection is to point out the dam foundation problem facing with serpentinization stage and testing their strength. And then all of collected samples from field study are preparation of thin section for microscopic analysis. And also, photographic records are made on hand specimens of the serpentinite rocks. Point load test was attempted to know the serpentine rock strength, but it failed. Because of the lower strength nature of serpentine rocks, this testing failed. Although the point load test failed, uniaxial compressive strength test was successful. The location map of the Yazagyo dam site for serpentinite samples was drawn by the aid of computer. After the preparation of thin section, detailed petrological analysis was made by Olympus binocular microscope. After the analysis of thin section, those were photomicrographed not only under the Plane Polarize light but also Cross Nicols. In this study, the serpentinite minerals are identified and figured according to the serpentinite identification chart for thin section as adopted by Wick and Whittaker (1977). All of the identified samples and thin section numbers in this thesis are prefixed by- YZS (Yazagyo Serpentinite).

3.2 Types of serpentinites in the area and their occurrence

Three types of serpentine can be distinguished in this area, (a) Massive serpentine (b) Sheared serpentine (c) Vein serpentine (cross fibre and slip fibre). It consists essentially of antigorite, lizardite, bastite with magnetite and chromite as accessory minerals. Differentiations of these minerals are made after Wicks and Whittaker (1977). Three types of serpentine classified with respect to textural variations are shown in Table (1).

Table 1. Textural variations of the serpentinite

Texture	Minerals
Pseudomorphic Texture Mesh rim Mesh centre Hourglass	Magnetite with Antigorite Antigorite with Magnetite in center Antigorite, Lizardite, Bastite
Non-Pseudomorphic Texture Interlocking Interpenetrating Serrated veins	Antigorite Antigorite Chrysotile
Vein Serpentine Cross-fiber Slip-fiber	Chrysotile asbestos Chrysotile asbestos

3.2 Massive serpentine

In outcrop, these have a smoother surface with yellowish brown to pale greenish brown in color and yellowish brown to pale greenish brown color. Fresh surface of both serpentinites are dark greenish black in colour and both are massive in nature. These type of serpentine are located mostly in left bank of Neyinzaya stream (Fig-2), power house (Fig-3). In microscopic studies, these types of serpentine are dominantly shown in Mesh texture and interpenetrating nature. The predominant minerals are Antigorite and Bastite. The antigorite are shown in thorn shape and hourglass structure in the serpentinite, which consists of 45-60 % (Fig-4). The Bastite shown rounded shaped, those are 15-25% constitute in thin section. The cross-fiber veins are sometime occurring with 3-5%. The Magnetite and chromites is present in minor amounts with 4-8%. These are shown opaque and irregular outline under the microscope (Fig-5). However, their nature and percentage is very important for determination of the degree of serpentinization. Magnetite is mostly found within the mesh rims of antigorite. These massive type serpentinite are mainly confined to the partially serpentinized zone.



Fig 2. Massive type of Serpentine, left bank of Neyinzaya stream, (G.P.S loc- 23° 32' 10"N, 94° 05' 30"E), Facing NE

3.3 Sheared serpentine

The types are the results of tectonic movements in places, for example, along fault zones. They are mostly found as vertical cliffs and they are also called "fish scale serpentine", Cooke (1937). This type is

characterized by its smooth shiny surfaces and variations in shades range from dusty yellow-green through grayish-green to pale green or yellow-green. In the study area, along the northern flanks of Talone Hill (Fig-6) and right banching wall of spillway construction are well exposed in this types of serpentine. In microspocic study, this type of serpentine is shown in hourglass texture with interlocking (Fig-7) and interpenetrating. The predominant minerals are antigorite and Chrysotile. The antigorite has shown hourglass texture with 60-75%. However, they are never found alone and are usually found in combination with interpenetrating or interlocking textures. Chrysotiles are seen as small cross veins with 25-35% (Fig-8). Some are cutting the other minerals. Magnetite is very fine grained with sub-parallel and disseminated grains in the hourglass texture. Mostly these are found as sub-rounded to sub-rectangular shape.

3.4 Vein serpentine (cross-fiber and slip-fiber)

It is developed as numerous veins that may be on a microscopic or megascopic scale. This type of serpentine can be found along the joint planes. Some slip-fiber serpentine may be originally been cross-fibre that was deformed and recrystallized during shearing. Their color is commonly pale green to pale yellow green color with pearly luster (Fig-9). In microscopic study, this type of serpentine is shown in cross-fibre and locally sub-interpenetrating. The predominant minerals are Chrysotiles and antigorite. The Chrysotiles in which tiny veins follow the lines of weakness like parting and show as cross-fiber and slip-fiber nature. The cross-fiber veins are usually containing magnetite grains and sometime passes through the bastite (Fig-10). The slip-fiber veins here are arranged in such a way that these lie parallel or subparallel to the enclosing walls of the veins (Fig-11).



Fig 3. Massive type of Serpentine, at the power house site, (G.P.S loc- 23° 32' 28"N, 94° 05' 06"E), Facing-East

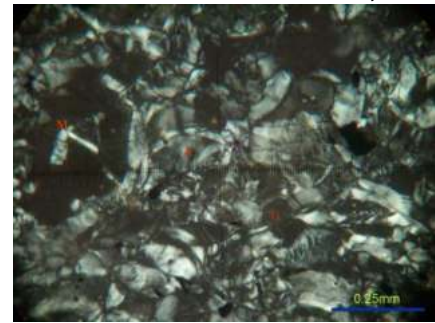


Fig 4. Hourglass texture, Bastite (B); Antigorite (A), Magnetite (M). Sample- (YZS-D) (G.P.S loc- 23° 32' 51"N, 94° 05' 25"E), between XN

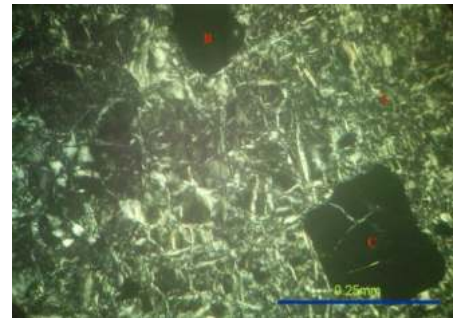


Fig 5. Chromite (C) grain shown in opaque and replaced by serpentine along the cracks, A is Antigorite, B is Bastite (G.P.S loc- 23° 31' 28"N, 94° 05' 18"E), between XN



Fig 6. Shear type of serpentine, northern flank of Talone Hill, (G.P.S loc- 23° 31' 49"N, 94° 05' 18"E), Facing-SW



Fig 7. Interlocking texture in antigorite, sample no- (YZS-M) (G.P.S loc- 23° 32' 29"N, 94° 05' 39"E), between XN



Fig 8. Chrysotiles are seen as small cross veins, sample no-(YZS-B) (G.P.S loc- 23° 32' 18"N, 94° 06' 09"E), between X.N



Fig 9. Serpentine with chrysotile asbestoses, core sample from UCH-7, RD-3970ft, 6.5ft.

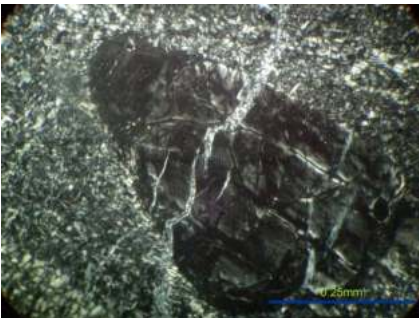


Fig 10. Chrysotile cross-fiber vein are passed through the bastite, (G.P.S loc-23° 32' 30"N, 94° 05' 40"E), between X.N

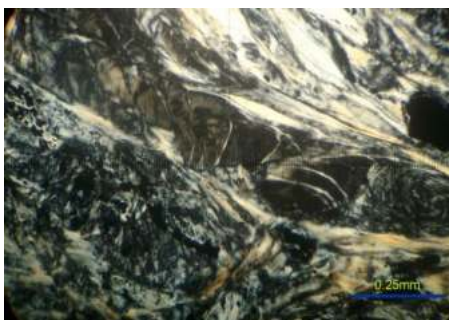


Fig 11. Parallel to subparallel nature of slip-fiber vein, (G.P.S loc- 23° 31' 51"N, 94° 05' 25"E), between X.N

4. ARBITRARY ZONAL ARRANGEMENT OF SERPENTINES

Two zones are recognized in the serpentinite body of Yazagyo Multipurpose Dam site project (Fig-12). Depending on the degree of alteration they are classed as; (a) Partially serpentized Zone (I)

TULSOJRI

(b) Completely serpentized Zone (II).

Each zone bears its characteristic textures as shown in Table (2)

Table 2. Zonal arrangement of serpentinites in Yazagyo Multipurpose Dam site with their respective textures, structure and relic minerals

Texture	Structure	Relic minerals	Completely serpentized Zone	Partially serpentized Zone
Non Pseudo-morphic	-	-	Most abundant	Nil
Pseudo-morphic	-	-	Present	Most abundant
-	vein	-	Traced	Most abundant
-	-	Olivine	Traced	Nil

4.1 Partially serpentized zone (I)

Pseudomorphic (mesh rimmed and mesh centered) and vein serpentinite especially Chrysotile asbestoses (cross-fiber veins and slip-fiber veins) textures, are commonly observed distinctly in relic of olivine (Fig-13). The shapes of mesh are sub-square to square shapes and some are sub-square to triangular form (Fig-14). In mesh texture, two portions may be considered separately, the mesh rim and mesh center. Most of the mesh rims are possibly antigorite. Mesh centers are usually lizardite. Frequently relic olivine is found as mesh centre. Magnetite is found as discrete fine grains throughout this zone.

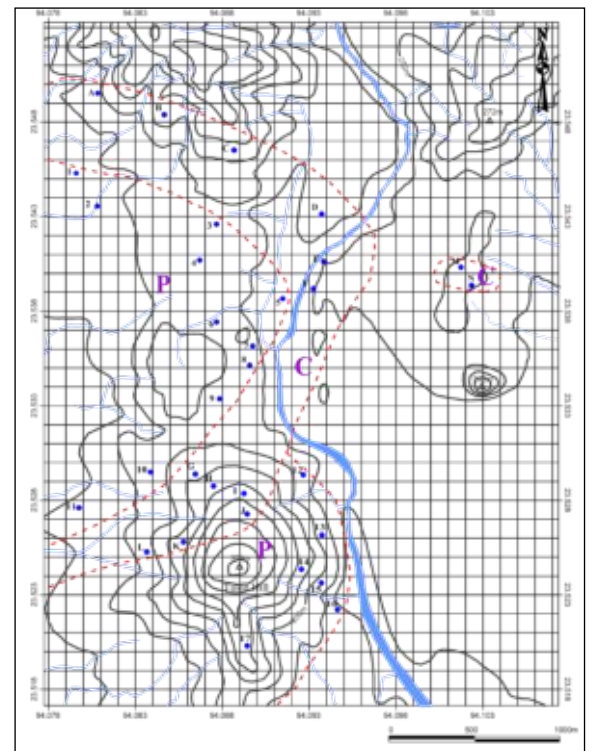


Fig 12. Serpentine samples location and Arbitrary zonal arrangement in the Yazagyo Dam site project area with reference to the degree of serpentization.

(I). P- Partially serpentization zone

(II). C- Completely serpentinization zone (1, 2, 3-- , 17 and A, B, C---, N -serpentinite samples location)

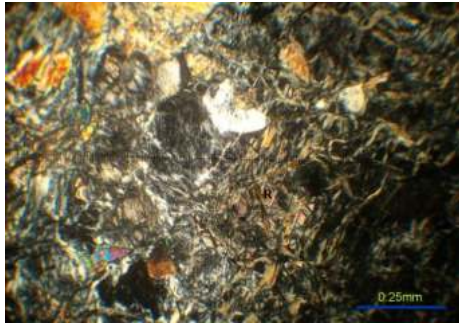


Fig 13. Relic olivine grains in the mesh structure. Sample no-15, (G.P.S loc- 22° 31' 34.3"N, 94° 05' 43"E), between X.N

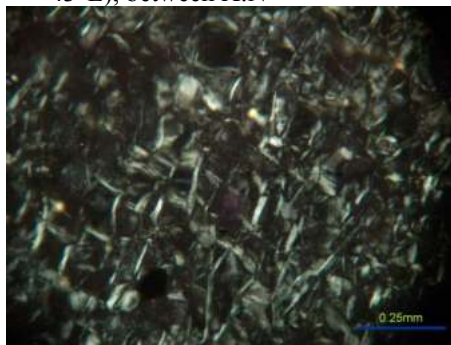


Fig 14. Mesh texture showing various outline, Sample no- 4, (G.P.S loc- 23° 32' 25"N, 94° 05' 18"E), between X.N

4.2 Completely serpentinized zone (II)

Pseudomorphic texture like mesh texture (mesh rimmed, mesh centred) (Fig-15) and hourglass structure are quite common in bastite and antigorite of this zone (Fig-16). Non-Pseudomorphic textures of interlocking and slip-fibre veins are also observed (Fig-18). These are exposed at or near the saddle Dam II. Mesh textures show variants in outline, square, equilateral or even triangular (Fig-15). Such textures are sometimes found at the rims or otherwise centred. Frequently relic olivine is found as mesh centres or concentrated small disseminated grains, and sometime large amounts with granular form. Magnetite is found as large amount.

4.3 Engineering Geological Problem of Serpentine Foundation

As the left and right abutment of main dam axis is situated at the landslide area, it is very difficult to excavate and foundation treatment is due to the weak mechanical properties of serpentine. Serpentinites are already highly fractured and sheared, weather to produce plastic clay capable of holding a great amount of moisture. Disintegration and remolding produce a clayey soil with little shear strength that can be found as the seat of sliding for landslide in serpentinite area of Talone Hill. Moreover, the main dam axis is located in the debris and slope wash deposits of Talone Hill and Khamauk Hill in which the thickness of the deposit is up to 18m deep. Fresh bed rocks are not observed according to the bore

holes data. Also this area is partially serpentinite zone at the right abutment of the dam site, especially eastern flank of Talone Hill according to petrological studies. Saddle II and Right abutment of the main dam axis is very close to local thrusting which is trending NNW-SSE. Dolerite intrusions also cause the serpentinite rock into fracture rocks. Hence, seepages are also noted. Completely serpentinization zone are more stable than partially serpentinization zone. The partially altered serpentinite areas are geologically unstable region because of their mineral composition, such as relic olivine and other serpentine minerals. These are altered by weathering and any geological phenomenon. Moreover the relicts of olivine are lower resistance to weathering in Bowen's reaction series. If these types of serpentine are directly contact with water, these are react with water and facing with volume change, and then forced to form of chrysotile vein lets. These vein lets are possible to formed weak zone.



Fig 15. Mesh texture (mesh rimmed, mesh centred). Sample no-J, (G.P.S loc- 23° 31' 46"N, 94° 05' 21"E), between X.N



Fig 16. Hourglass structure and thorn shaped antigorite in the serpentinite. Sample no- D, (G.P.S loc- 23° 32' 25"N, 94° 05' 18"E), between X.N



Fig 17. Slip-fiber vein in the serpentinite. Sample no-G, (G.P.S loc- 23° 31' 48"N, 94° 05' 19"E), between X.N

4.4 Uniaxial compressive strength of the serpentine (σ_c)

The uniaxial compression strength test was carried out on four serpentine rock core samples. The test results showed the uniaxial compressive strength has 14 MPa, 14.2 MPa, 15.3 MPa and 14.8 MPa respectively. The first two are resulted of the partially serpentinized samples and the others are completely serpentinized samples. The mode of failure is shown in (Fig-18). This result reveals that the strength of serpentine rocks is very low strength, according to Deere and Miller's intact rock strength classification. The strength of these serpentine rocks are not really precise with laboratory testing after, Cappell and Maurice (1980), so these rock are should be measured with some in-situ methods such as plate bearing test, groundmass and block ratio, and Elastometer test etc.



Fig 18. Failure of serpentine core sample, after the UCS testing.

5. CONCLUSIONS

During the field investigation, serpentine samples were systematically collected to revise the serpentinization stages and to test for rock strength in laboratory. Three types of texture are observed in thin sections: pseudomorphic, non-pseudomorphic and vein. The relict minerals indicate that the original rock was mainly peridotite. In general, the degree of serpentinization may be regarded as partial to nearly complete. Two zones of serpentinization are delineated on a map for the serpentinite body. These are (a) P zone - partial serpentinization zone, (b) C zone - complete serpentinization zone. The engineering properties of serpentine rocks are tested by point load test and uniaxial compressive strength test. Due to the nature of serpentine rock, the real value of RQD and compressive strength cannot be measured in usual way of measuring of other rocks. Therefore, the strength of these rocks is measured with some insitu tests such as plate bearing test, and Elastometer test etc. Due to the nature of partial

serpentinization, dam abutment should be changed to complete serpentinization zone.

ACKNOWLEDGEMENT

We would like to express my deepest gratitude to Part time Professor Dr. Ohn Thwin from Yangon University, Department of Geology for his excellent guidance, caring, patience and providing us with an excellent atmosphere for doing research. We also would like to thank former Associate Professor Dr Kyaw Htun from Yangon Technological University, Engineering geology Department for his useful comments, remarks and engagement through the doing research. Special thanks go to Ministry of Education, Department of Higher Education (Lower Myanmar) for permission to carry out this research and providing research funds (2015-16 Fiscal Year, Maubin University). The first author would never have been able to finish research without the guidance of my supervisor, help from friends, and support from my parent. The first author would like to thanks U Aung Moe Kyaw (Site Manager, Singapore) who as a good friend was always willing to help and his best suggestions.

REFERENCES

- [1] Bowen, N.L & Tuttle, O.F. The system $MgO-SiO_2-H_2O$, *Bull-geol-Soc-Amm* vol. 60, 439-460pp, 1949.
- [2] Cappell, A.B. and Maurice, R., Classification of Rock Mass Related to Foundation. *Proc. Of Inter.Cont. on structural foundation on rock, Sydney*.27-32pp, 1980.
- [3] Coats, C.J.A., Serpentine minerals from Manitoba. *Can Mineral.* Vol 9, 322-347pp, 1968.
- [4] Cooke, H.C, Thetford, Disraeli and eastern half of Warwick map areas, Quebec. *Geol. Surv. Can. Mem.* 211p. 1937.
- [5] Goodman, R.E. *Engineering Geology: Rock in Engineering Geology*. John Wiley & Sons, INC 412p. 1993.
- [6] Kyaw Htun, Tint Lwin Swe, Kyaw Aung and Htun Htun Aung, Engineering Geology of Upper Buywa Multipurpose Dam Project. Unpublished technical report. Submitted to Irrigation Department, 17p. 2007.
- [7] Kyaw Htun, Kyaw Aung and Ohn Thwin, Geological Site Report of the Yazagyo Dam Site. Unpublished technical report. Submitted to Irrigation Department, 15p.2009.
- [8] Wicks, F.J and Whittaker, E.J.W. Serpentine textures and serpentinization. *Canadian Mineralogist* vol.15, 459-488pp. 1977.

Comparative Study on Seismic Response of RC Structure Using Viscous and Viscoelastic Dampers

Su Myat Aye⁽¹⁾, Dr Kyaw Moe Aung⁽²⁾, Dr Hla Myo Aung⁽³⁾

⁽¹⁾Technological University (Sagaing), Myanmar

⁽²⁾ Technological University ((Kyauk Se), Myanmar

⁽³⁾Technological University (Sagaing), Myanmar

Email: {sumyataye61116, kyawmoeaung07, hlamyoaung.aung}@gmail.com

ABSTRACT: This paper presents comparative study on seismic response of fifteen-storey reinforced concrete building using viscous dampers and viscoelastic dampers. The proposed building is located in Mandalay, seismic zone 4. It is a L-shaped building and its occupancy is residential. All structural members are designed according to ACI 318-99. Load consideration is based on UBC-97. The frame type of proposed building used is the special RC moment resisting frame. In this study, response spectrum analysis method is used for dynamic analysis. The analysis and design of structure is carried out by using ETABS v 9.7.1 software. In this study, viscous dampers and viscoelastic dampers are used to control seismic response of the proposed building. The mechanic properties of viscous damper used in this study are $C_d=320(\text{kN}/(\text{mm/s})^\alpha)$ and stiffness $K_d=224(\text{kN}/\text{mm})$. The mechanic properties of viscoelastic damper used in this study are $C_d=12(\text{kN}/(\text{mm/s}))$ and stiffness $K_d=57(\text{kN}/\text{mm})$. The storey drifts, storey shears, storey moments, point displacements and storey accelerations are compared.

KEYWORDS: *Seismic Response, Earthquakes, Viscous Damper, Viscoelastic Damper.*

1. INTRODUCTION

Myanmar is a developing country and population rate is surprisingly increasing. The proposed building is located in Mandalay, the second largest city of Myanmar. It is considered high seismic hazard because Mandalay situates near the Myanmar's largest active fault, the Sagaing fault. So, it is necessary to design safe structures which can safely withstand earthquakes of reasonable magnitude. The high-rise is essentially a vertical cantilever so that the elements of structure are designed; to resist axial loading by gravity and to resist transverse loading by wind and earthquake. Seismic design of building structures is based on the concept of increasing the resistance capacity of the structures against earthquakes by employing, the use of shear walls, based frames, or moment-resistant frames. Conventional seismic design attempts to make building that do not damage during minor earthquake, moderate earthquakes

with negligible structural damage and some non structural damage and major earthquakes with some structural and non structural damage. The main goal of earthquake resistant design is to attain a structure with sufficient strength and ductility to assure life safely. Nowadays, three basic technologies are used to protect buildings from damaging earthquakes effects. These are base isolation, passive energy dissipation devices and active control devices. In the past several decades, a variety of passive energy dissipation devices have been developed, such as oil dampers, viscoelastic dampers, metallic dampers, and friction dampers, etc. Passive energy dissipation devices and, in particular, dampers incorporating viscous and viscoelastic materials have been introduced in civil engineering structures for seismic applications. The objective of the study is to compare analysis results of member forces of reinforced concrete structure using viscous and viscoelastic damper.

2. PASSIVE ENERGY DISSIPATION DEVICE

2.1 Viscous Damper

Most various dampers are fluid dampers, similar to the shock absorbers in automobiles. Viscous dampers of varieties of materials and damping parameters were proposed and developed for seismic protection. Viscous fluid dampers commonly used as passive energy dissipation devices for seismic protection of structures are principally composed of a piston rod, a piston head and a cylinder filled with a viscous fluid. Fluid viscous dampers which operate on the principle of fluid flow through orifices are installed in a number of structural applications. Example of construction of viscous fluid viscous damper is shown in Figure 1.

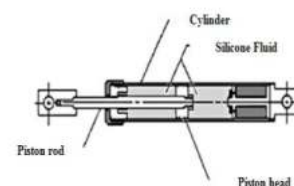


Fig 1. Example of construction of Viscous Fluid Damper

Viscoelastic materials used in structural applications are usually copolymers or glassy substances that dissipated energy through shear deformation. These materials have an elastic stiffness, with a displacement dependent force, as well as a viscous component which produces a velocity dependent force. Bitumen rubber compound can also be used, as the viscoelastically material, in the energy absorbing device. Viscoelastic damper are made of viscoelastically layers connected with steel plates. Energy dissipation is achieved in these layers, by shear deformation which occurs as different components move relatively to each other. Example of construction of viscous fluid damper is shown in Figure 2.

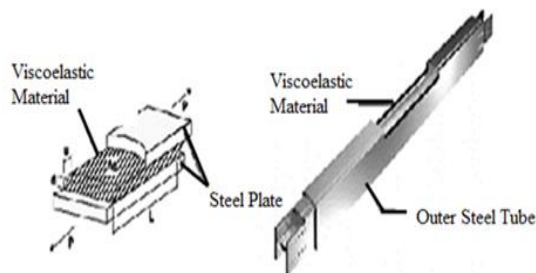


Fig 2. Example of construction of Viscoelastic Damper

3. MODEL PREPARATION

3.1 Data for Proposed Structure

The structure is fifteen-storeyed, L-shaped reinforced concrete residential building. The structure has two normal stairs and two elevators.

Type of structure = Fifteen-storey R.C building,

Type of occupancy = Residential, two units in each floor

Length of structure = 120ft

Width of structure = 92ft

Ground floor height = 12ft

Typical story height = 10ft

Stair roof height = 7ft

Overall height = 169ft

Line plan of proposed damped structure are shown in Figure 3.

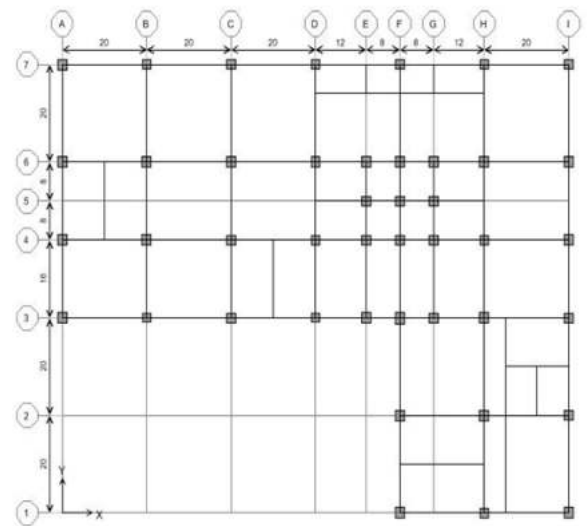


Fig 3. Line Plan of Proposed Structure

3.2 Material Properties of the Structure

Weight per unit volume of concrete = 150pcf

Specified concrete compressive strength, f'_c = 3ksi

Bending reinforcement; yield stress, f_y = 50ksi

Bending reinforcement; yield stress, f_s = 50ksi

Modulus of Elasticity, E_c = 3122ksi

Poisson's ratio, μ = 0.2

3.3 Loading Consideration and Load Combinations

The applied loads considered in this structural analysis such as dead loads, live loads, earthquake load and wind loads are based on UBC-97. Design codes applied are ACI 318-99 and UBC-97. There are fourteen number of load combinations which are used in the structural dynamic analysis.

1. 1.4 DL
2. 1.4 DL + 1.7 LL
3. 1.05 DL + 1.275 LL + 1.275 WX
4. 1.05 DL + 1.275 LL - 1.275 WX
5. 1.05 DL + 1.275 LL + 1.275 WY
6. 1.05 DL + 1.275 LL - 1.275 WY
7. 0.9 DL + 1.3 WX
8. 0.9 DL - 1.3 WX
9. 0.9 DL + 1.3 WY
10. 0.9 DL - 1.3 WY
11. 0.614 DL + 1.43 SPECX
12. 0.614 DL + 1.43 SPECY

13. 1.3305 DL + 1.275 LL + 1.4025
SPECX

14. 1.3305 DL + 1.275 LL + 1.4025
SPECY

3.4 Structural Stability

The superstructure is needed to check for overturning moment, sliding and storey drift for stability of proposed buildings.

In checking for overturning, the ratio of resisting moment to overturning moment of the proposed damped structures (the factor of safety) is greater than 1.5. So, the overturning moment checking is safety. The factor of safety for sliding is greater than 1.5. Therefore, there is no sliding occur in the structure. In checking for storey drift, it is found that storey drift for all storeys do not exceed limit. Therefore, the proposed building is satisfied for all stability check.

3.6 Structural Elements For Proposed structure

Beam sizes and column sizes of the proposed reinforced concrete building structure with undamped case, damped case with viscous and with viscoelastic dampers are described in this study. Beam sizes are 10"x12", 10"x14", 10"x16", 12"x14", 12"x16", 12"x18", 14"x18", 14"x20", 14"x22", 14"x24", 16"x18", 16"x20", 16"x22", 16"x24", 18"x18", 18"x20", 18"x22", 18"x24", 20"x22", 20"x24", and 22"x24". Column sizes are 20"x20", 22"x22", 24"x24", 26"x26", 28"x28" and 30"x30". Slab thickness is 5" for all slabs and waist thickness is 7".

4. COMPARASION OF DYNAMIC ANALYSIS RESULTS

Analysis results of three cases of proposed structure are compared in this paper. Comparison of storey drift, storey shear, point displacements and acceleration are described under controlled load case for SPECX and SPEC Y.

Comparison of storey drifts in X and Y directions are shown in Table I, Figure 4 and Table II, Figure 5 respectively.

TABLE I. STOREY DRIFT IN X DIRECTION (UNIT-IN)

Storey	Storey Drifts in X direction		
	Without damper	With Viscoelastic damper (VED)	With Viscous damper (VD)
SR	0.000953	0.000726	0.000526
R	0.001033	0.00078	0.000583
15	0.001489	0.001031	0.000754
14	0.001902	0.001324	0.000941

13	0.002205	0.001567	0.001107
12	0.00233	0.001703	0.001193
11	0.002465	0.001853	0.001289
10	0.002518	0.001946	0.001345
9	0.002426	0.001921	0.00132
8	0.002272	0.001829	0.001253
7	0.00229	0.001855	0.001269
6	0.002349	0.001894	0.001295
5	0.00241	0.001913	0.001305
4	0.002372	0.001838	0.001247
3	0.002354	0.001753	0.001177
2	0.002187	0.001431	0.000899
1	0.001292	0.000554	0.000168

TABLE II. STOREY DRIFT IN Y DIRECTION (UNIT-IN)

Storey	Storey Drifts in Y direction		
	Without damper	With Viscoelastic damper (VED)	With Viscous damper (VD)
SR	0.000784	0.00071	0.000521
R	0.00114	0.000873	0.000702
15	0.001705	0.001286	0.001059
14	0.002253	0.001706	0.001379
13	0.002719	0.00209	0.001619
12	0.002917	0.002284	0.001675
11	0.00317	0.002527	0.001753
10	0.00334	0.002711	0.001777
9	0.003295	0.002718	0.001692
8	0.003082	0.002569	0.001541
7	0.00316	0.002644	0.001563
6	0.003276	0.002734	0.001623
5	0.003385	0.002803	0.001693
4	0.003331	0.002732	0.001682
3	0.003316	0.00269	0.001678
2	0.003075	0.002452	0.001522
1	0.001835	0.001419	0.000856

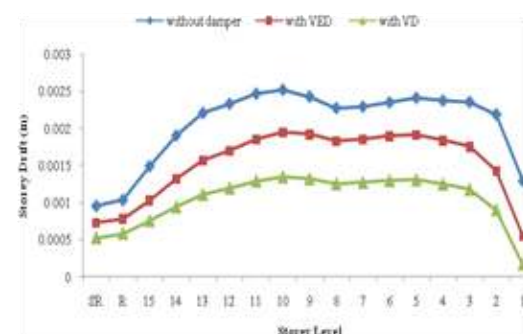


Fig 4. Comparison of storey drift in X direction

1	1483.7	1001.42	156.78
---	--------	---------	--------

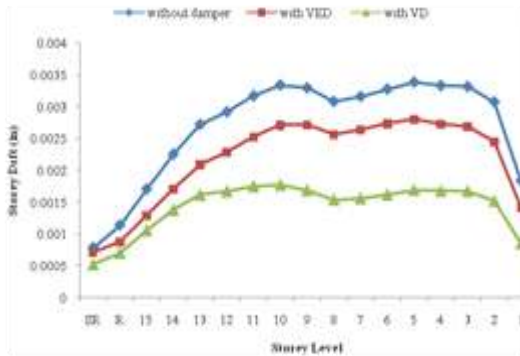


Fig. 5 Comparison of storey drift in Y direction

Comparison of storey shears in X and Y directions for SPECX and SPECY are shown in Table III, Figure 6 and Table IV, Figure 7.

TABLE III. STOREY SHEARS IN X DIRECTION (UNIT - KIP)

Storey	Storey Shear in X direction		
	<i>Without damper</i>	<i>With Viscoelastic damper (VED)</i>	<i>With Viscous damper (VD)</i>
SR	15.59	10.78	8.67
R	206.23	142.39	112.6
15	402.34	280.97	217.54
14	563.95	398.96	301.9
13	693.9	499.99	371.48
12	800.06	589.92	433.17
11	887.87	671.08	488.95
10	960.18	742.92	538.05
9	1023.83	807.16	582.08
8	1088.93	867.86	624.4
7	1158.84	924.97	664.73
6	1230.94	976.73	701.44
5	1301.38	1022.17	734.37
4	1367.33	1061.22	763.81
3	1424.41	1092.09	787.35
2	1464.83	1110.95	800.43

TABLE IV. Storey shears in y direction (unit - kip)

Storey	Storey Shear in Y Direction		
	<i>Without damper</i>	<i>With Viscoelastic damper (VED)</i>	<i>With Viscous damper (VD)</i>
SR	15.9	14.55	10.01
R	213.11	189.94	141.15
15	410.76	366.77	277.47
14	565.82	504.31	388.19
13	687.98	610.73	474.28
12	791.73	701.02	540.8
11	882.36	783.15	592.06
10	958.08	856.3	630.82
9	1023.53	921.55	663.49
8	1089.57	984.48	699.14
7	1159.49	1046.54	742.12
6	1228.96	1105.61	790.56
5	1294.63	1161.26	840.72
4	1357.05	1215.3	889.59
3	1414.87	1266.36	933.25
2	1459.26	1305.97	965.09
1	1481.86	1326.41	980.84

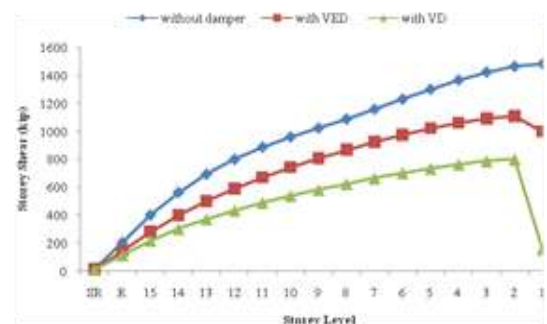


Fig 6. Comparison of storey shear in X direction

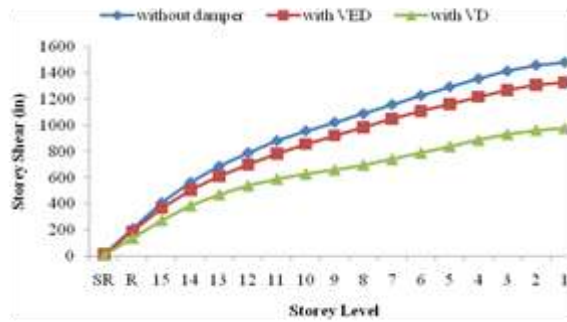


Fig 7. Comparison of storey shear in Y direction

Comparison of point displacements in X direction for SPECX and SPECY are shown in Table VII , Figure 8 and Table VIII, Figure 9 respectively.

TABLE VII. Point Displacement in x direction (unit-in)

Storey	Point Displacement X Direction		
	<i>Without damper</i>	<i>With Viscoelastic damper (VED)</i>	<i>With Viscous damper (VD)</i>
SR	3.73	2.9272	1.959
R	3.63	2.8463	1.9024
15	3.48	2.7315	1.8222
14	3.30	2.5853	1.7206
13	3.08	2.4108	1.6001
12	2.85	2.2198	1.4688
11	2.60	2.01	1.3253
10	2.34	1.7869	1.1733
9	2.08	1.5643	1.0218
8	1.83	1.3512	0.8767
7	1.57	1.1321	0.7273
6	1.29	0.9067	0.5736
5	1.01	0.6785	0.418
4	0.73	0.4587	0.2686
3	0.44	0.2485	0.1277
2	0.18	0.0772	0.0218
1	3.73	2.9272	1.959

TABLE VIII. Point Displacement in y direction (unit-in)

Storey	Point Displacement Y Direction		
	<i>Without damper</i>	<i>With Viscoelastic damper (VED)</i>	<i>With Viscous damper (VD)</i>
SR	5.01	4.2505	2.5155
R	4.90	4.1534	2.4488
15	4.73	4.0113	2.3527
14	4.50	3.8231	2.2301
13	4.23	3.5908	2.0861
12	3.93	3.3343	1.9348
11	3.60	3.0474	1.7728
10	3.24	2.7363	1.6026
9	2.88	2.4211	1.4324
8	2.54	2.12	1.2682
7	2.18	1.8074	1.0937
6	1.80	1.4822	0.9063
5	1.41	1.1474	0.7067
4	1.01	0.8203	0.5061
3	0.62	0.4978	0.3053
2	0.26	0.2036	0.1229
1	5.01	4.2505	2.5155

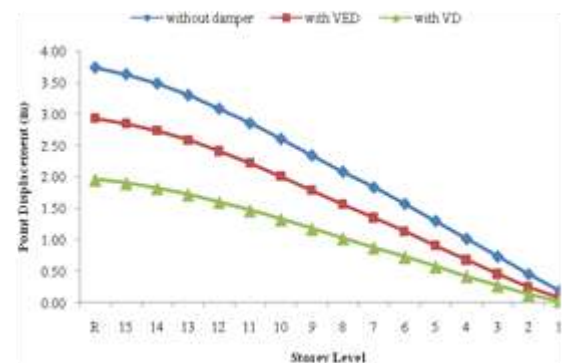


Fig 8. Comparison of point displacement in X direction

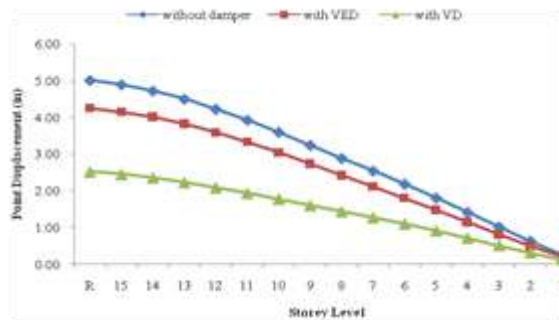
TABLE X. Storey Acceleration in Y direction (unit-in/Sec²)

Fig 9. Comparison of point displacement in Y direction

Comparison of storey acceleration in X direction for SPECX and SPECY are shown in Table IX , Figure 10 and Table X, Figure 11 respectively.

TABLE IX. Storey Acceleration in X direction (unit-in/Sec²)

Storey	Storey Acceleration in X Direction		
	Without damper	With Viscoelastic damper (VED)	With Viscous damper (VD)
SR	67.2053	43.5758	36.6792
R	73.5879	48.2796	42.2127
15	64.1736	41.2311	33.9891
14	53.6105	37.0441	26.7348
13	46.2089	33.7127	25.0501
12	42.7034	31.1214	25.5489
11	41.6153	29.1899	24.9001
10	43.2005	28.3928	25.249
9	47.1555	30.8023	27.5472
8	50.6193	33.059	29.1287
7	51.6007	33.2824	28.798
6	50.7286	32.7916	28.4576
5	48.6496	32.5778	28.8852
4	44.6344	31.1833	27.6206
3	37.3256	26.3657	22.122
2	26.3347	17.6044	12.4768
1	12.1714	7.0722	2.711

Storey	Storey Acceleration in Y Direction		
	Without damper	With Viscoelastic damper (VED)	With Viscous damper (VD)
SR	63.1956	58.3786	41.668
R	96.6319	66.1917	63.0177
15	86.0925	61.5754	54.1371
14	74.0363	56.0722	44.1082
13	65.7581	51.3859	37.7818
12	61.5986	47.8106	35.122
11	59.3041	45.0972	34.2058
10	59.2318	43.3435	36.2311
9	62.0216	42.7391	41.1416
8	64.9958	42.388	45.2759
7	65.3972	41.1484	46.3193
6	63.9245	38.9296	45.4478
5	61.4759	40.0396	43.6585
4	56.9398	41.0674	40.1056
3	48.1382	37.5438	33.2014
2	33.7334	27.6747	22.3299
1	15.4612	13.1578	9.5677

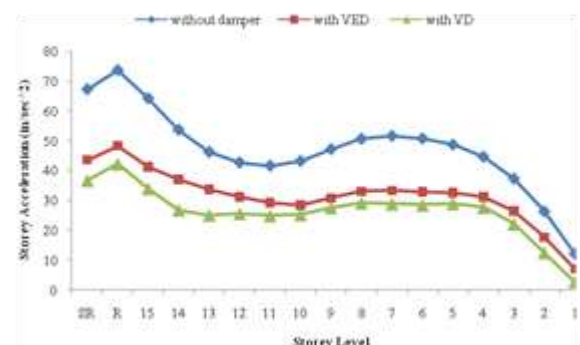


Fig 10. Comparison of storey acceleration in X direction

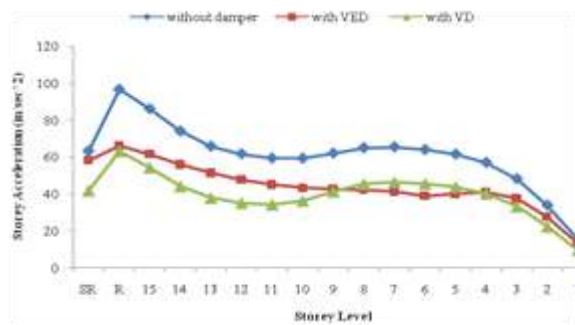


Fig 11. Comparison of storey acceleration in Y direction

4. DISCUSSION AND CONCLUSIONS

In this study, viscous and viscoelastic dampers are used to reduce seismic response of the structure subjected to the earthquake loads. The dimensions of the proposed fifteen-storey RC building are 120 ft long, 92 ft wide and the overall height is 169 ft. The proposed building is located in seismic zone 4. The material properties are concrete compressive strength, $f_c' = 3000$ psi and $f_y = 50000$ psi. For the dynamic analysis, the response spectrum analysis method is used. The design of superstructure is checked with overturning effects, sliding resistance, and storey drifts. Viscous and viscoelastic damper are installed only U2 direction at the base storey of the structure. In the comparison of results of the structure with viscoelastic damper and the structure without damper, reduction in storey drifts ranges between 23% to 24% , storey shears between 11% to 32%, point displacement between 15% to 21% for structure with viscoelastic damper. Moreover, storey accelerations are about 15% and 49% less than that of uncontrolled structure.

In the comparison of storey drifts in X and Y directions, storey drifts in the structure with viscous dampers are about 50% less than that of undamped structure. In comparison of storey shears in X and Y direction, storey shears in structure without damper are about 50% greater than that of structure with viscous damper. Moreover in comparison of point displacement in X and Y directions of structure, point displacements of structure with viscous damper are 50% less than that of the structure without viscous damper. Reduction in storey accelerations occur about 50% for structure with viscous damper.

In comparison of three cases of proposed structure, viscous dampers are the most effective in reducing seismic response of the structure. Therefore, it can be seen that adding viscous dampers and viscoelastic damper to the structure reduces not only the deformation but also the storey shear. It can be concluded that seismic response can be reduced by adding dampers in the structures.

ACKNOWLEDGEMENT

The author is very thankful to Dr. Aung San Lin, Pro-Rector of Technological University (Sagaing), for his in valuable permission and support in carrying out this paper. The author would like to express special thanks to Dr. Kyaw Moe Aung, Professor and Head of Department of Civil Engineering, Technological University (Kyaukse) for his grateful encouragement, continued patience and true-line guidance.

The author wishes to record his thanks to Dr. Hla Myo Aung, Professor and Head, Department of Civil Engineering, Technological University (Sagaing), for his guidance, suggestions and necessary advice. Finally, the author would like to express grateful thanks to all teachers and her parents for their supports, kindness and love.

REFERENCES

- [1] Arthur H. Nilson: *Design of Concrete Structure* Twelfth Edition, McGraw-Hill, Inc.(1997)..Arthur H. Nilson: *Design of Concrete Structure* Twelfth Edition, McGraw-Hill, Inc.(1997)..
- [2] (1997), Uniform Building Code, Volume 2, U.S.A, *Structural Engineering Design Provisions*, International Conference of Building Officials.
- [3] American Concrete Institute 1999: *Building Code Requirement for Structural Concrete (318-99)*. U.S.A
- [4] ETABS Version 9.7.1 "Computers and Structures", Inc; Berkeley; California.
- [5] [7] Fu, Y. and Kasai, K. (1998). Comparative study of frames using viscoelastic and viscous damper *Journal of Structural Engineering*. 124:5. 513- 522.

Comparative Study on Seismic Response of Dynamic Analysis Methods on RC Building

Kyi Pyar Khaing ⁽¹⁾, Dr. Hla Myo Aung ⁽²⁾, Chan Nyein Moe Oo Nge ⁽³⁾

⁽¹⁾Technological University (Sagaing), Myanmar

⁽²⁾Technological University (Sagaing), Myanmar

⁽³⁾Technological University (Sagaing), Myanmar

Email: kyipyarkhaing2@gmail.com

ABSTRACT: This paper describes the comparative study seismic response of dynamic analysis methods on reinforced concrete building. The proposed building is located in seismic zone IV and the overall height is 107 ft. Gravity and lateral loads are considered based on ASCE7-10. All structural members are designed according to ACI 318-14. For the analysis of the building, the ETABS software (version 16.0.0) is used. After static stability checking is carried out, the proposed building is analyzed with response spectrum analysis (RSA) and time history analysis (THA). The seismic response such as story drifts, story shears of RSA and THA are compared. The comparative results of axial and shear forces of columns are investigated for dynamic analysis methods.

KEYWORDS: *ASCE7-10, ACI 318-14, response spectrum analysis, time history analysis, seismic response*

1. INTRODUCTION

Myanmar is still a developing country and there is a tendency to raise population in future. The requirements of increased population and natural geology of country highly demands the high-rise building. For severe earthquake region of Myanmar, it is likely to meet highly destructive damage of earthquake to the buildings in these areas. Therefore, high-rise building should be designed to resist the earthquake effects. The behavior of a building doing an earthquake depends on several factors, stiffness, adequate lateral strength, ductility, simple and regular configurations. The buildings with regular geometry and uniformly distributed mass and stiffness in plan as well as in elevation suffer much less damage compared to irregular configuration. But nowadays, need and demand of the latest generation and growing population has made the architects or engineers inevitable towards planning of irregular configurations.

Many buildings are being constructed with irregular configuration both in plan and elevation. This in future may subject to devastating earthquakes. In case, it is necessary to identify the performance of the structures to withstand again disaster for both new and existing one. The static analysis is not enough to get adequate structural response data (story shear, story drift and story displacement) of the building. So, the buildings are needed to analyze and design by using

dynamic analysis. In this study, irregular-shaped RC building is analyzed with two dynamic analysis methods and the seismic response and comparative results are presented.

2. OBJECTIVES OF THE STUDY

The objectives of the study are as follow;

- (1) To analyze the proposed building with response spectrum analysis and time history analysis.
- (2) To investigate the analysis results of the proposed building.
- (3) To compare the seismic response of dynamic analysis methods.

3. DATA PREPARATION FOR THE PROPOSED BUILDING

3.1 Site Location and Structural Configuration

Site Location and Structural Configuration are listed as follows:

Location	: Seismic zone IV
Type of Building	: Eighth-storyed Irregular-shaped RC Building
Type of Occupancy	: Residential
Plan Dimension	: X direction = 80 ft Y direction = 45 ft
Height of Building	: 107 ft
Typical Story Height	: 11 ft
Bottom Story Height	: 11 ft
Depth of Foundation	: 10 ft

3.2 Material Properties

The strength of a building depends on the strength of the materials.

➤ Analysis property data

Modulus of elasticity, E_c = 3122 ksi

Poisson's ratio, ν = 0.2

Coefficient of thermal expansion = 5.5×10^{-6} in / in per degree F

➤ Design property data

Bending reinforcement yield stress (F_y) = 50 ksi

Shear reinforcement yield stress (F_{ys}) = 50 ksi

Concrete cylinder strength (f_c) = 3 ksi

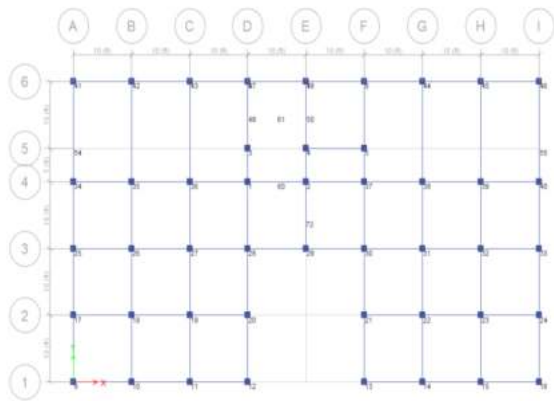


Fig 1. Floor Plan for Proposed Building

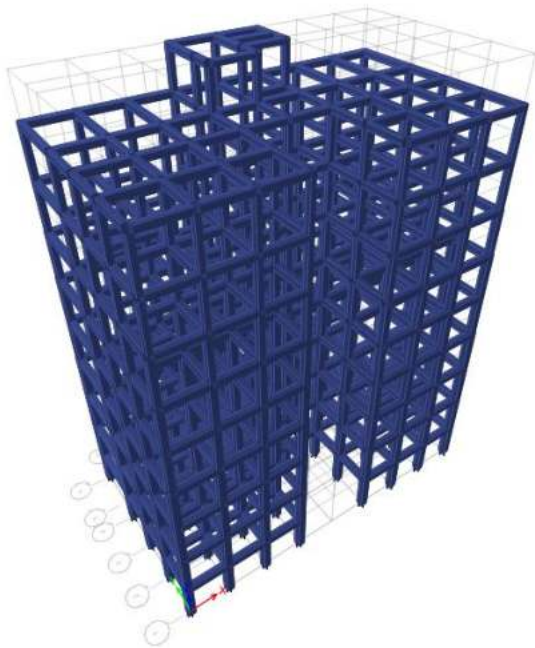


Fig 2. 3D View for Proposed Building

3.3 Load Consideration

There are two kind of loads considered in this study which is gravity load, that include dead and live load, lateral load that include wind and earthquake load.

(1) Dead Load

Dead loads consist of the weight of all material and fixed equipments incorporated into the building. Required data for dead loads are as follows:

Superimposed dead load = 25 psf

9" thick wall weight = 100 psf

4.5" thick wall weight = 55 psf

Weight of elevator (including person weight) = 3 tons

(2) Live Load

Live loads are gravity load produced by the used and occupancy of the building and do not include dead loads, construction load, or environmental loads such as wind and earthquake loadings are based on ASCE7-10. Required data for live loads are as follows:

Live load on private rooms = 40 psf

Live load on stair case = 100 psf

Live load on roof floor = 20 psf

Weight of water = 62.4 pcf

(3) Wind Load

The wind pressure on a structure depends on the wind response of the structure. Required Data in designing for wind load are as follows:

Basic wind speed, V = 80 mph

Surface Roughness = Type B

Exposure type = Type B

Wind important factor, I = 1

Gust effect factor, G = 0.85

Topographic factor, K_{zt} = 1

Wind Directionality Factor, K_d = 0.85

(4) Earthquake Load

Required data for earthquake Load are as follows:

Type of Seismic zone = Zone IV

Seismic zone factor, Z = 0.4g

Seismic design category = D

Site class (soil type) = D

Important factor, I = 1

Spectral response acceleration parameters

for 0.2s, S_s = 2.01

Spectral response acceleration parameters

for 1.0s, S_1 = 0.8

Approximate period parameter, C_t = 0.016
 $\alpha = 0.9$

Response modification factor, R = 8

System overstrength factor, Ω_o = 3

Deflection amplification factor, C_d = 5.5

4. LOAD COMBINATIONS

The design load combinations are the various combinations of the load cases for which the building needs to be checked. These combinations are based on ACI 318-14 and ASCE7-10. They are as follows:

- (1) 1.4DL
- (2) 1.2DL+ 1.6LL
- (3) 1.2DL + 1.0LL + 0.5WX
- (4) 1.2DL + 1.0LL - 0.5WX
- (5) 1.2DL + 1.0LL + 0.5WY
- (6) 1.2DL + 1.0LL - 0.5WY
- (7) 1.2DL + 1.0LL + 1.0WX
- (8) 1.2DL + 1.0LL - 1.0WX
- (9) 1.2DL + 1.0LL + 1.0WY
- (10) 1.2DL + 1.0LL - 1.0WY
- (11) 1.2DL + 1.0LL + 1.0EX
- (12) 1.2DL + 1.0LL - 1.0EX
- (13) 1.2DL + 1.0LL + 1.0EY
- (14) 1.2DL + 1.0LL - 1.0EY
- (15) 0.9DL + 1.0 WX
- (16) 0.9DL - 1.0 WX
- (17) 0.9DL + 1.0 WY
- (18) 0.9DL - 1.0 WY
- (19) 0.9DL + 1.0EX
- (20) 0.9DL - 1.0EX
- (21) 0.9DL + 1.0EY
- (22) 0.9DL - 1.0EY

where,

- DL = dead load
 LL = live load
 WX = wind force in X-direction
 WY = wind force in Y-direction
 EX = earthquake load in X-direction
 EY = earthquake load in Y-direction

5. STABILITY CHECKING OF THE PROPOSED BUILDING

The proposed building is firstly analyzed by static case. Stability checking of the proposed building for static analysis such as (1) overturning, (2) sliding, (3) story drift, (4) torsional irregularity and (5) P-Δ effect are within the limit.

Table 1. Safety Value of Structural Stability

Checking	Safety Factor Value		Limit	Remark
	X-direction	Y-direction		
Overturning	7.34	4.37	1.5	Satisfied
Sliding	3.24	3.3	1.5	Satisfied
Story Drift	2.3232	2.6136	2.64	Satisfied
Torsional Irregularity	1.03	1.01	1.2	Satisfied
P- Δ Effect	0.0429	0.0491	0.1	Satisfied

6. DYNAMIC ANALYSIS METHODS

After checking the stability, the proposed building is analyzed with response spectrum analysis (RSA) and time history analysis (THA). Response spectrum method is the linear dynamic analysis method. In this method the peak structural response can be obtained directly during an earthquake using the earthquake responses (or design) spectrum. Time History method is step by step analysis of the dynamic response of the structure at each time increment when its base is subjected to ground motion time history record. To perform such an analysis a representative earthquake time history is essential for a structure being evaluated.

7. COMPARISON OF ANALYSIS RESULTS WITH RESPONSE SPECTRUM ANALYSIS AND TIME HISTORY ANALYSIS

In this study, the seismic response such as story drifts, story shears of response spectrum analysis and time history analysis are compared in Figures 3 to 6. And the comparisons of axial and shear forces of columns are presented in Figures 7 to 18. Columns are typically chosen as corner, exterior and interior columns.



Fig 3. Story Drift X due to EX

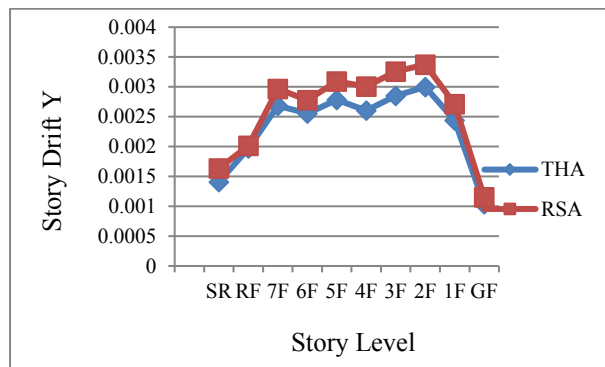


Fig 4. Story Drift Y due to EY

The peak value in story drift X and Y due to EX and EY can be resulted at 2F of the proposed building for both RSA and THA. From the above figures, story drifts for RSA are 40.8% and 12.5% more than that for THA. So, the structural results of RSA give more significant seismic response of the proposed building for the dynamic analysis.

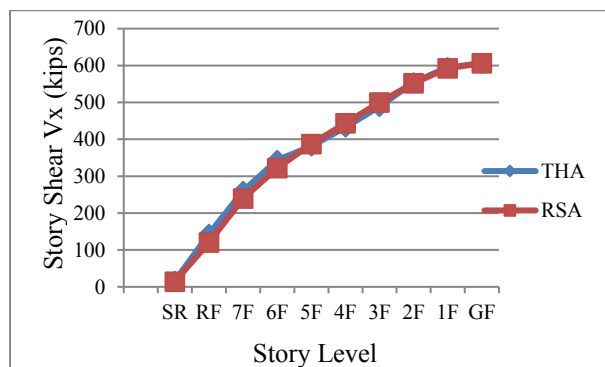


Fig 5. Story Shear Vx due to EX

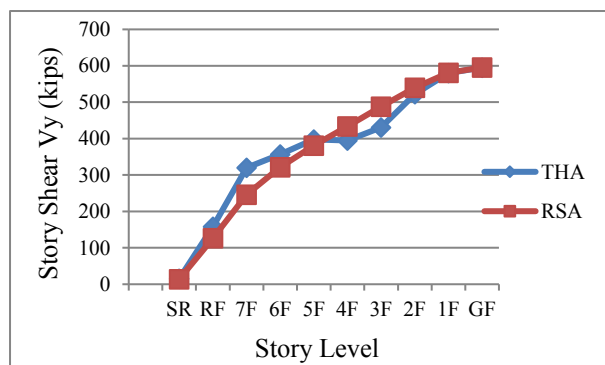


Fig 6. Story Shear Vy due to EY

Figures 5 and 6 describe the comparison of story shears of RSA and THA. The horizontal line presents the story level and the vertical line presents story shears in kips respectively. Story shears of THA are less than 0.05% and 0.03% for X and Y directions at GF than that of RSA.

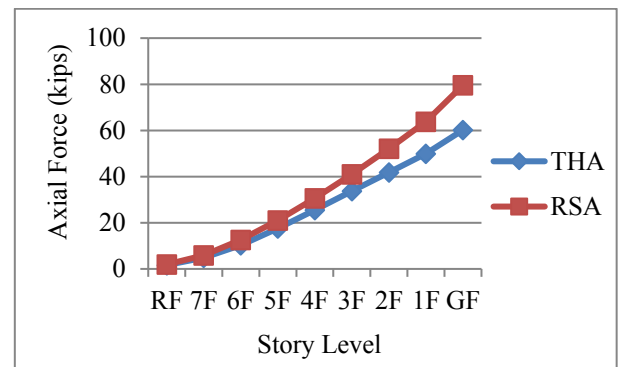


Fig 7. Axial Force due to EX for Corner Column

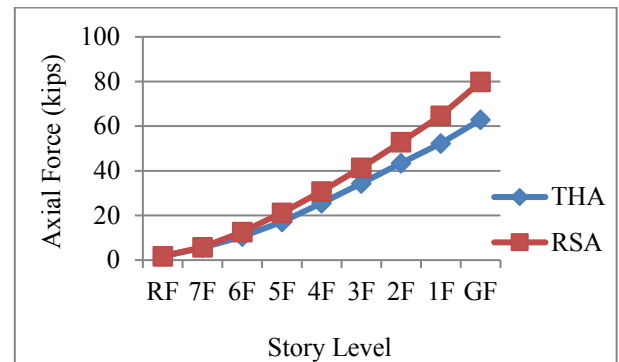


Fig 8. Axial Force due to EX for Exterior Column

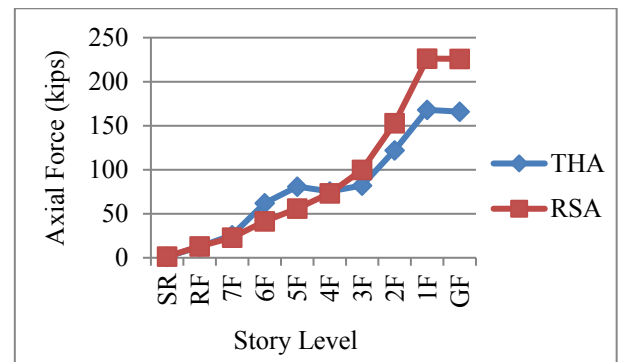


Fig 9. Axial Force due to EX for Interior Column

According to above figures, the gradual increase in axial forces is found in corner and exterior columns for both THA and RSA. It can be seen that more obvious increase in axial force for interior column of RSA than 34.7% that of THA at 1F.

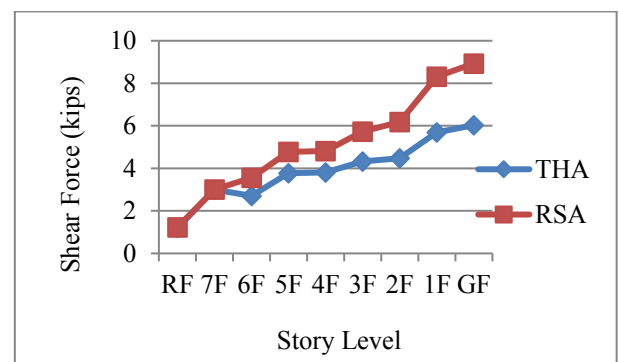


Fig 10. Shear Force due to EX for Corner Column

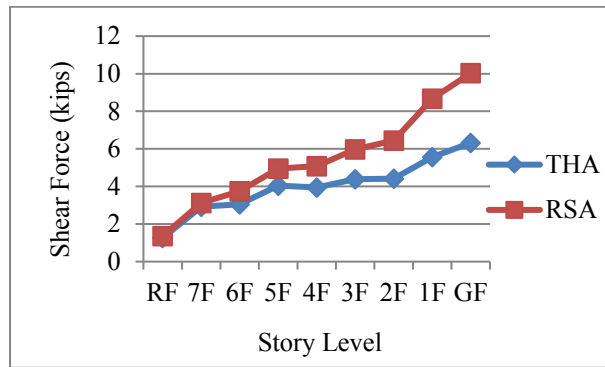


Fig 11. Shear Force due to EX for Exterior Column

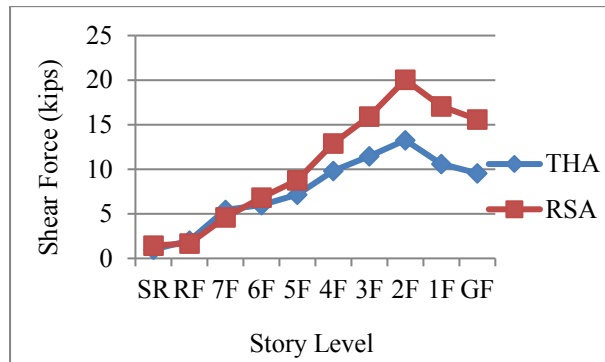


Fig 12. Shear Force due to EX for Interior Column

According to Figures 10 to 12, there is a significantly fluctuate in shear forces of columns at 2F and 6F due to EX. The obvious difference about 51% between RSA and THA can be seen at 2F for the interior column of proposed building.

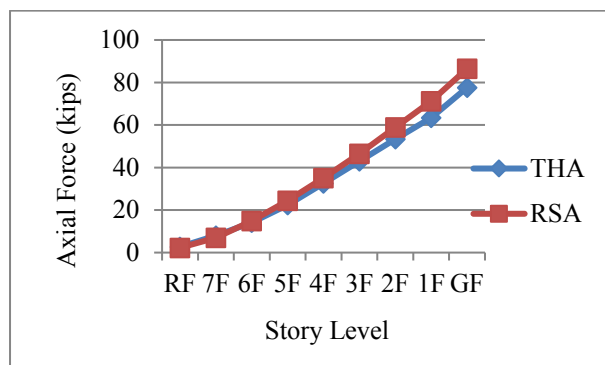


Fig 13. Axial Force due to EY for Corner Column

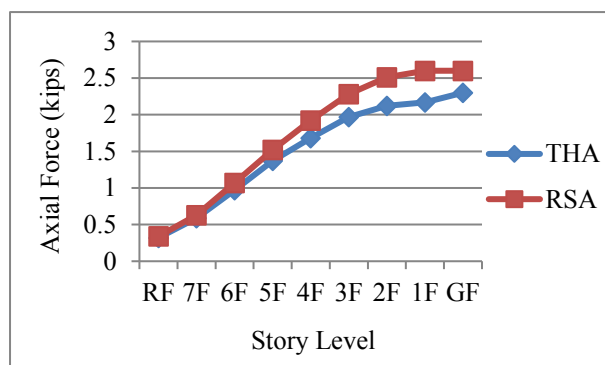


Fig 14. Axial Force due to EY for Exterior Column

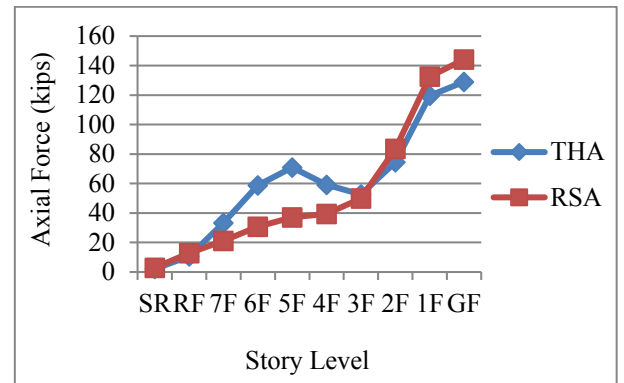


Fig 15. Axial Force due to EY for Interior Column

According to above figures, the significant increase in axial forces is found in corner and exterior columns due to EY for both THA and RSA. It can be observed that more fluctuated change about 47.8% in axial force for interior column of RSA and THA at 5F.

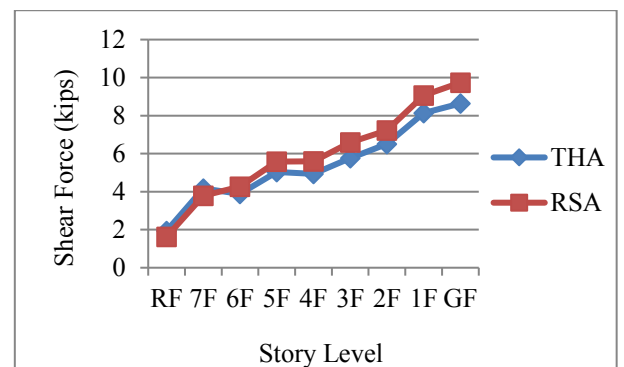


Fig 16. Shear Force due to EY for Corner Column

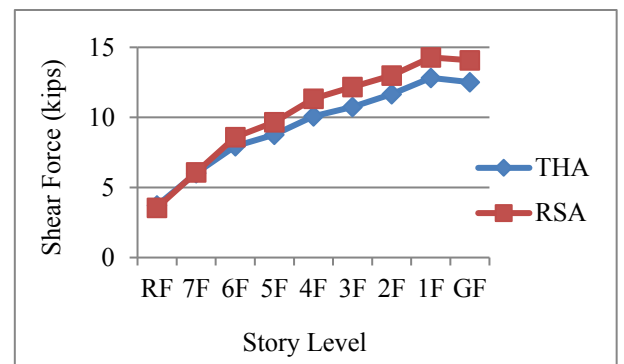


Fig 17. Shear Force due to EY for Exterior Column

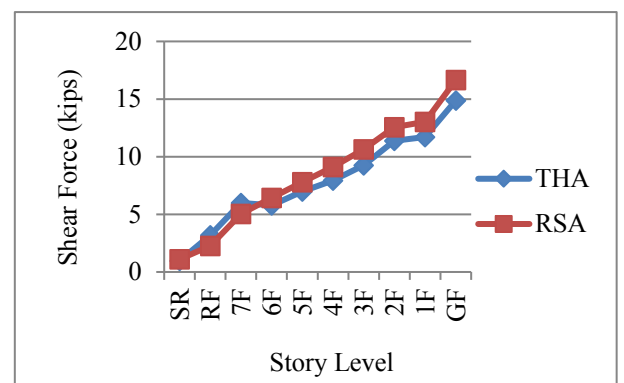


Fig 18. Shear Force due to EY for Interior Column

From the above Figures 16 to 18, comparative results of RSA and THA for columns due to EY can be known for dynamic analysis of the proposed building. There is a considerable change about 14.4%, 13.3% and 14.8% of RSA and THA in columns for shear forces due to EY.

8. CONCLUSION

In this paper, the comparative study on dynamic analysis methods of the eighth-storyed irregular-shaped RC building is presented. After the stability checking is satisfied, the proposed building is analyzed with RSA and THA and the analysis results are compared. The seismic response such as story drift and shear for RSA are found to be more than THA. The peak value in story drift X and Y due to EX and EY can be resulted at 2F of the proposed building for both RSA and THA. Moreover, axial and shear forces of corner, exterior and interior columns for THA results less than RSA. The considerable change of RSA and THA in columns for axial and shear forces due to EY can be investigated from this study. The obvious difference about 51% between RSA and THA can be seen in interior column at 2F for EX due to the configuration of the proposed building. So, RSA shows more significant seismic response compared with THA and causes high stresses in structural members especially columns.

ACKNOWLEDGEMENT

The author is very thankful to Dr. Aung San Lin, Pro-Rector of Technological University (Sagaing), for his in valuable permission and kind support in carrying out this research. The author wishes to record her thanks to Dr. Hla Myo Aung, Professor and Head, Department of Civil Engineering, Technological University (Sagaing), for his guidance, suggestions and necessary advice. The author also wishes to thank all her friends for their helps and advices on her studying. Finally, the author would like to express grateful thanks to all teachers and her parents for their supports, kindness and unconditional love.

REFERENCES

- [1] Atul N.Kolekar, "Comparative study of Performance of RCC Multi-Storey Building for Koyna and Bhuj Earthquakes", Journal of Engineering Research and Application, Volume 7, Issue 5, (Part -2) May 2017, pp.45-52.
- [2] Prakriti Chandrakar, "Comparison between Response Spectrum Method and Time History Method for Dynamic Analysis of Multistoried Building", International Journal of Science and Research (IJSR), Volume 6, Issue 5, May 2017.
- [3] American Concrete Institute, Building Code Requirements for Structural Concrete (ACI 318-14), U.S.A.
- [4] American Society of Civil Engineers Minimum Design Loads for Buildings and Other Structures (ASCE7-10).
- [5] "ETABS version (16.2.1)", Computer & Structure Inc.

Lithostratigraphy of Thitsipin Formation in Singaung Area, Pindaya Township, Southern Shan State, Myanmar

Thant Sin⁽¹⁾ & Thidar Theint⁽²⁾

⁽¹⁾Associate Professor, Department of Geology, Bago University

⁽²⁾ Assistant Lecturer, Department of Geology, Dagon University

geol.thantsin@gmail.com

ABSTRACT: The study area is situated at the Singaung village, Pindaya Township, Southern Shan State. The base map refers to one-inch topographic map of 93 D/9. The area extent is square 30 miles. The purposes of these research is based on stratigraphy of a detail geological map, systematic lithostratigraphic classification of rock units, and petrographic description of rock. In method of study, field investigation was mainly based on the numerous traverses and detailed section measurements. Representative sample were collects during the section measurement. The area is mainly covered by older Paleozoic rock. Coarse dendritic and centripetal pattern are presented in the study area. Sinkholes and fault scarps are also presented. The major lithology of study area is limestone, dolomites, siltstones and shale. The exposed rock units are Wunbye Formation (Middle Ordovician), Nan-on Formation (Late Ordovician), Linwe Formation (Early Silurian) and Thitsipin Formation (Middle Permian). The Thitsipin limestone is composed of very thick bedded to massive, bluish grey limestone, rugose and tabulae corals bearing micritic and arenaceous limestone, dolomitic limestone, lithographic limestone, calcitic limestone and brecciated limestone which is exposed at highly mountain and karst topography. The fossils, Tabulae and Rugose Corals, *Ipciphyllum sp.*, *Wentzellophyllum*, *Syringopora*, *Thomasiphyllum sp.*, and *Iranophyllum*, Crinoids stem, Gastropods, Brachiopods, Bryozoan, *Fenestella*, and other shell fragments which are observed in Thitsipin Formation. According to Folk's classification the carbonate rock units of the Plateau Limestone Group are commonly biosparites, pelsparite, pelmicrite, intrasparite and dolostone.

KEY WORDS: Thisipin Formation, limestone, coral, biosparite

1. INTRODUCTION

1.1. Location, Size and Accessibility

The study area, Singaung is situated at Pindaya Township, Southern Shan State. The investigated area is bounded by latitude from (20°54' 7") to (20°57' 25") N and longitude from (96° 38' 00") to (20°40' 52") E. The area can be accessible from Aungban to Pindaya town by the

car. Anyone can be easily reached because Pindaya Town is situated beside Pindaya-Heho main road see in Figure (1).

1.2. Topography and Drainage

The area lies in the Shan Plateau region. Topographically, the mountain ranges are rugged, consisting several peaks and gorges. In the study area, there are two different topographic features. The western parts of the area are mountainous terrains. The western part is higher than the eastern part. The clips and scarps are found on the highest mountain ranges in the western part. Sinkhole and karst topography can be found in the Wunbye limestone and Plateau limestone areas. Fault scarps, ponds and springs are found in the area because they are related to the fault. Figure (2) shows topographic nature of the investigated area. Some streams are fault-controlled streams and they give centripetal, dendritic and sub-angular drainage patterns. Centripetal, sinkholes are in western part, fine dendritic pattern in southern and southeastern parts and coarse dendritic pattern occur in northeastern part. Figure (3) shows drainage pattern of the investigated area.

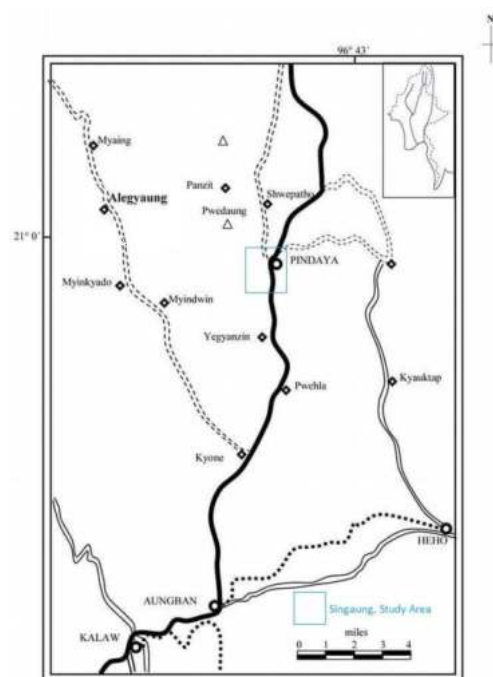


Figure (1) Location Map of the study area

1.3 Purpose of Study

The study was undertaken with special aim of the presentation of the stratigraphy and structure of the part of Singaung area, Pindaya Township. In the course of study, preparation of a detail geological map, a systematic lithostratigraphic classification of rock units, petrographic description of rock, geological structures and correlation with the geology of adjacent areas.

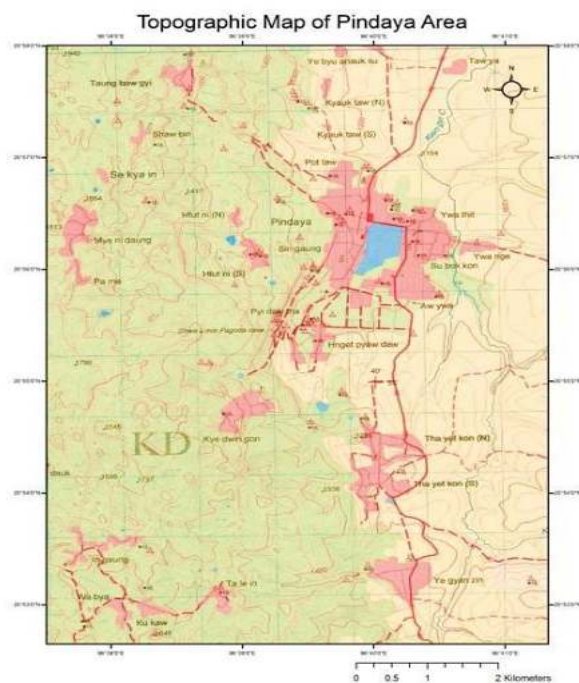


Figure (2) Topographic Map of the study area

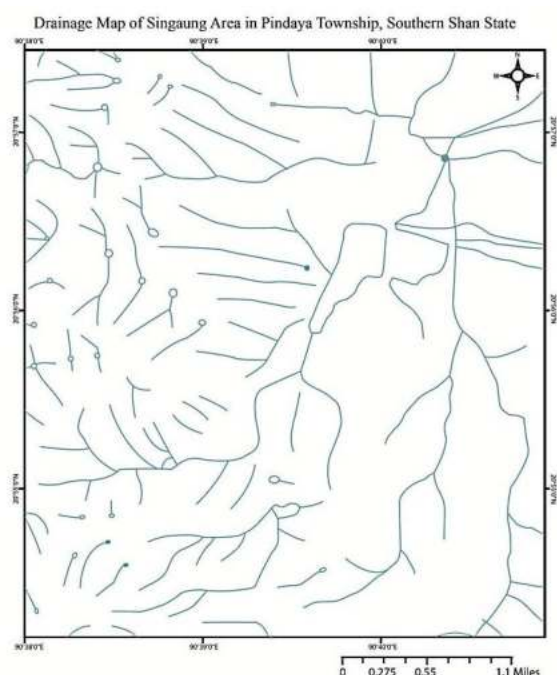


Figure (3) Drainage Map of the study area

1.4. Method of Study

Before going out to the study area, the aerial photographs were studied by using mirror stereoscope to demarcate the lithostratigraphic boundaries, the trends of outcrops, possible structural features such as fold, fault and other fractures. Then, photogeological features were checked and corrections were done by the field evidences.

Field investigation was mainly based on the numerous traverses and detailed section measurements. The structural data and field descriptions were recorded in field note. Formation boundaries, fossil localities, sedimentary structure and economic mineral occurrence were directly plotted on the base map. Detailed section measurements were done along the area, where the tectonic effects were minimums. Representative samples were collected during the section measurement.

1.5. Previous Work

The Paleozoic sediments occupy as a chief component of the Pindaya range. The Paleozoic rocks of Pindaya range had been studied by many geologists, according to the aspects of mineralization, stratigraphy and paleontology.

The geologists of the Geological Survey of India (G.S.I) was the foremost investigator of Myanmar Paleozoic Pindaya range.

Brown (1931) was the first to describe the systematic regional geology of the Paleozoic rock of the Southern Shan State, and drew the first geological map on the quarter inch scale.

Brown and Scandhi (1933) revised Brown's earlier paper and map to bring the geologic, paleontologic and stratigraphic data.

Reed (1932,1936), Elles and Wood (1936) described some paleontologic accounts of the Southern Shan State.

Brown and Sondhi's work is monumental, and no such significant paper was published since then, except brief accounts given by Sandhi in Heron's General Reports (1935), (1936). Above Fact.

Above facts were incorporated in the textbooks written by Chhibber (1935) and Pascoe (1959).

Dr. Myint Lwin Thein et al. (1972), described and established the succession and lower Paleozoic stratigraphy of the western part of the Southern Shan State.

2. REGIONAL GEOLOGY

2.1. Regional Stratigraphy

The present area is located at the North-eastern margin of the Pindaya range. It lies in the Eastern Highland of Myanmar. This area is composed of clastic sediments and carbonate sediments. The stratigraphic units exposed in the study area are Wunbye Formation (Middle Ordovician), Nan-on Formation (Upper Ordovician), Linwe Formation (Lower Silurian), Wabya Formation (Middle Ordovician) and Plateau Limestone (Permian to Triassic) with nearly north-south trend.

The Wunbye Formation is mainly composed of grey to bluish grey limestone fine to medium grained size and buff pinkish silt patches and burrows structure and siltstone are buff and yellow and laminated nature. Dolomitic limestones are dark colour thick bedded often massive and highly jointed surface in criss-crossed pattern.

The Non-on formation is mainly consists of siltstones, mudstones and marl, siltstone are thin to medium bedded, buff and orange colour and mudstone are light grey colour, fine to medium grained size.

The Linwe Formation is mainly composed of light grey phacoidal limestone, argillaceous limestones, shales, calcareous mudstones, purplish colour phacoidal limestone and greenish grey micaceous siltstone.

The Wabya Formation is mainly consists of shales, slaty shales and slates, shales is light grey to white, thin to medium bedded. Slaty shales and slate are black.

The Thitsipin limestone crops out mostly in isolate but widely scattered patches with distinctive rugged, craggy topography surrounded mostly by smoother terrain underlain by the Plateau limestone Group (Nwabangyi Dolomite).

3. FINDINGS AND DISCUSSION:

LITHOSTRATIGRAPHY

3.1. General Statement

The Southern Shan State is situated on the Eastern part of Myanmar, as part of the Shan Plateau, which rises up to the general elevation of 4000 fts above sea level. This mountainous region continues north-westward into the terrains of Northern Shan State and Yunnan and Southward into the mountainous regions of the Kayah State. The Singaung area is located at the eastern limb of

south plunging Pindaya anticline of Southern Shan State. Lower Paleozoic unit of Pindaya Group, Mibayataung Group and upper Paleozoic unit of Plateau limestone are exposed in this study area which are as following see Figures (17 and 18) which are geological map and lithostratigraphic measured section of the study area (Singaung area).

3.2. Plateau Limestone Group

3.2.1. Thitsipin Formation

Name Derivation and Type Section

The name Thitsipin Limestone Formation was given by Garsonet.al (1976) to the limestone of Thitsipin village in Ye-ngan Township. This name was modified by Win Swe (1976) as Thitsipin Limestone.

Distribution

The Thitsipin limestone crops out mostly in isolate but widely scattered patches with distinctive rugged, craggy topography surrounded mostly by smoother terrain underlain by the Nwabangyi Dolomite. This formation unconformably overlies Silurian and other Paleozoic rocks. The Thitsipin Formation is well and wide exposed in the eastern part study area as a highly mountains.

Lithology

The Thitsipin limestone is composed of very thick bedded to massive, bluish grey limestone, rugose and tabulae coral bearing micritic and arenaceous limestone, dolomitic limestone, lithographic limestone, calcitic limestone and brecciated limestone which is exposed at highly mountain and karst topography see Figures 4, 5 and 6.



Figure (4) Brecciated limestone of Thitsipin Formation (near Htutni (North) village, North Facing)



Figure (5) Lithographic limestone of Thitsipin Formation (near Htutni (North) village, North Facing)



Figure (6) Fault breccia of Thitsipin Formation (Loc: 20°56' 42" N and 96° 38' 46"E, near Htutni(North) village, North-east Facing)

Stratigraphic Relationship

In the study area, this unit overlies unconformably the Linwe Formation of Early Silurian age and unconformably underlies the Quaternary alluvium.

Fossil Content

The fossils found in the Thitsipin limestone are Tabulae and Rugose Corals, *Ipciphyllum sp.*, *Wentzellophyllum*, *Syringopora*, *Thomasiphyllum sp.*, and *Iranophyllum*, Crinoids stem, Gastropods, Brachiopods, Bryozoan, *Fenestella*, and other shell fragments see Figures 7,8,9,10,11,12,13,14,15 and 16.



Figure (7) *Ipciphyllum sp.*, colonial rugose coral bearing micritic limestone of Thitsipin Formation (Loc: 20°56' 12" N and 96° 38' 50"E, near Htutni (North) village, west Facing)



Figure (8) *Ipciphyllum sp.*, colonial rugose coral bearing micritic limestone of Thitsipin Formation (Loc: 20°56' 12" N and 96° 38' 50"E, near Htutni (North) village, west Facing)



Figure (9) *Wentzellophyllum*, colonial rugose coral bearing micritic limestone of Thitsipin Formation (Loc: 20°56' 12" N and 96° 38' 50"E, near Htutni (North) village, west Facing)



Figure (10) *Syringopora*, tabulae coral bearing arenaceous limestone of Thitsipin Formation (Loc: 20°56' 12" N and 96° 38' 50"E, near Htutni (North) village, west Facing)



Figure (11) *Thomasiphyllum sp.* solitary rugose coral bearing arenaceous limestone of Thitsipin Formation (Loc: 20°56' 12" N and 96° 38' 50"E, near Htutni (North) village, west Facing)

Formation (Loc: 20°56' 02" N and 96° 39' 05"E, near Htutni (North) village, west Facing)



Figure (12) *Thomasiphyllum* sp. solitary rugose coral bearing arenaceous limestone of Thitsipin Formation (Loc: 20°56' 12" N and 96° 38' 50"E, near Htutni (North) village, west Facing)



Figure (13) *Iranophyllum*, solitary rugose coral bearing arenaceous limestone of Thitsipin Formation (Loc: 20°56' 12" N and 96° 38' 50"E, near Htutni (North) village, west Facing)



Figure (14) *Fenestella*, bryozoan bearing micritic limestone of Thitsipin Formation (Loc: 20°56' 32" N and 96° 38' 40"E, near Htutni (North) village, west Facing)

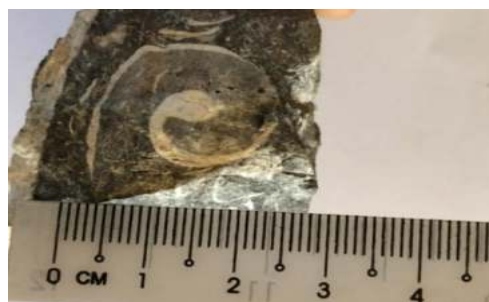


Figure (15) Gastropod coil bearing arenaceous limestone of Thitsipin Formation (Loc: 20°56' 32" N and 96° 38' 40"E, near Htutni (North) village, west Facing)



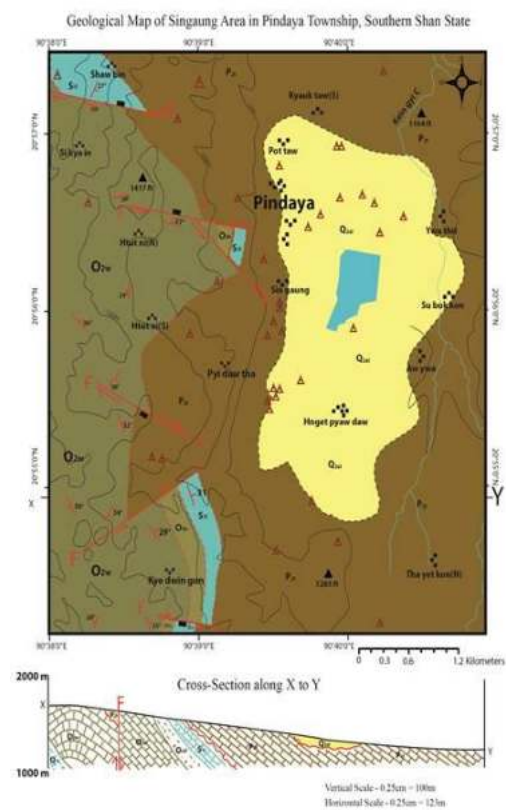
Figure (16) Gastropod coil bearing micritic limestone of Thitsipin Formation (Loc: 20°56' 32" N and 96° 38' 40"E, near Htutni (North) village, west Facing)

Age and Correlation






According to the basic of found faunal assemblage and stratigraphic position, the age of the Thitsipin Limestone is Middle Permian in age and it is assigned to be correlated with Tonbo limestone of Patheingyi Township Mandalay Division, Mawlamene limestone of Tanintharyi Division and Htan sang limestone of Southern Shan State.

Depositional Environment

The Thitsipin limestones were deposited under the shallow warm marine environment because it is carbonate environment and their content of coral.



Explanation

Stratigraphic Succession		Stratigraphic Symbol	Geological Age	Lithologic Description and Faunal Content
Group	Formation			
Pliocene-Lessons Group	Allevium	 Q _a	Quaternary	Recent Soil, Terrace Soil
	Thitspin Formation	 P _n	Middle Permian	The Thitspin formation is composed of very thick bedded to massive, bluish grey limestones, argillous and shaly sand bearing micritic and stromatolite limestones, dolomite limestones, siltylimestones, calcareous limestones and banded limestones which is exposed of highly limestone and karst topography.
	Lirwe Formation	 S _s	Early Silurian	Lirwe Formation consists of a succession of thin to medium bedded, purple, pink and grey colored subglobally columnar limestones with graphite bearing grey colored shale and yellow colored shstones and arenaceous limestones.
Pindaya Group	Nan-on Formation	 O _s	Late Ordovician	This unit mostly consists of thin bedded yellow to buff colored shstones or light orange calcareous limestone. Coarsely laminated limestones intercalated with shstones. In some study area, Nan-on Formation comprised thick laminated grey-white shstones. This formation is highly fossiliferous and with bedrock fossils.
	Wunbye Formation	 O _{on}	Middle Ordovician	Wunbye Formation is medium to thick bedded, light to dark grey and light purple limestones with shll lamination usually massive structure shl pindaya limestones. Some units with calcite veins (shlls and some are dolomitized). Algal laminated limestones, laminated limestones and calcite limestones are observed especially in three hills village.

Geographic Symbol

Structural Symbol












- | | | | |
|---|----------------|---|-----------------------------|
|  | - Pagoda |  | - Lithologic Contact |
|  | - Lake |  | - Fault |
|  | - Village |  | - Dip and Strike of bedding |
|  | - High Point |  | - Anticline |
|  | - Contour Line |  | - Syncline |
|  | - Stream | | |

Figure (17) Geological Map of Study Area (Singaung Area)

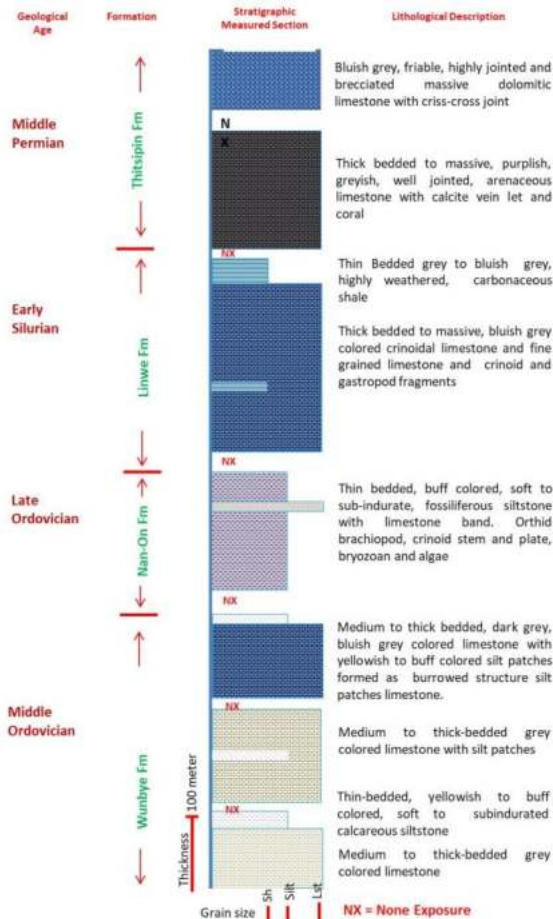


Figure (18) Lithostratigraphic Measured Section along Kyedwington village to west of Thayetgon village, from 20°54' 32" N and 96° 38' 42"E to 20°56' 32" N and 96° 39' 42"E

3.3. PETROGRAPHY OF CARBONATE ROCK UNITS

Lithostratigraphic units of study area have been recognized as Pindaya Group, Mibayataung Group and Plateau Limestone. For the petrographic study, some representative samples were collected from Wunbye Formation, Linwe Formation and Plateau Limestone Group. Then, thin-sections were prepared and studied under Petrographic Microscope and analyzed by visual estimation.

3.3.1. Petrography of Thitsipin Formation

In figure (19) petrographic thin section, Pellets occur in minor amount. These bioclasts and intraclasts grains commonly comprised about 33% to 37% of the total rock volume. Bioclasts are commonly range in size about 0.25mm to 1.0mm and are moderately sorted.

Intraclasts consist largely of elongated microcrystalline calcite. Silt-sized quartz grains, mica flakes and dark iron oxides are also formed. The Plateau Limestone Group consists of 20 to 34% of sparry calcite and 5 to 32% of microcrystalline calcite. Dolomites are well displayed in a major role upon the rocks of the Plateau Limestone Group. These crystals range from micron to centimicron size. Quartz contains 2 to 7% of the total rock volume. These are sub-angular to sub-rounded grains having size ranges from 0.02 to 0.2mm. They are well sorted grains. Generally, these quartz grains are commonly scattered. Muscovite mica and reddish brown to opaque iron oxide minerals are also present and they are commonly formed in the dolomitic layers of the Plateau Limestone Group. According to Folk's classification the carbonate rock units of the Plateau Limestone Group are commonly biosparites.



Figure (19) Microphotographic showing the micron to centimicron sized dolomite crystals in Thitsipin Formation. (Under PPL)

In figure (20) petrographic thin section, Pellets are the most abundant in Thitsipin Formation, ranging from 40 to 60% of the total rock volume. The shape of pellets is round, elongate and their sizes range from 0.02 to 0.5 mm in diameter.

The intraclasts, which constitute about 8%, are sub-angular to sub-rounded, moderately sorted and size of these intraclasts range from 1.75 to 5mm in length and 1.25 to 1.5mm in width. Bioclasts included in this formation are 5 to 10% by volume. Brachiopods, echinoderms, ostracods, gastropod, trilobite and mollusks are found as complete shells, or fragments. Molluscar shell fragments and echinoderm shell fragments are more abundant in this formation. The fossil fragments are poorly sorted. Their sizes and shapes are variable. Most sparry calcites occur as interparticle void-filling and sometimes also occur as intraparticle void-filling.

Sparite constitutes range from 10 to 25% of the total rock volume and their size ranges from 0.01 to 0.25 mm in diameter. Some void-filled sparry calcites have up to 1mm in diameter and it is called blocky calcite. Dolomite constitutes ranging from 20 to 25% of the total rock volume in the measured section. In the dolostone units, dolomite minerals vary from 60 to 90% of the total rock volume. Their size and shape are variable. Size of dolomite minerals are range from 0.04 to 0.25mm in diameter. Shapes of the single dolomites are ranging from euhedral to anhedral forms. The dolomites are characterized by iron oxide zonation.

Quartz and iron oxide grains are distributed throughout the Thitsipin limestones. Quartz grains, are moderately sorted, angular to sub-rounded forms consists never more than 5% by the total rock volume. According to Folk's classification, the Thitsipin limestone can be named as pelsparite, pelmicrite, intrasparite and dolostone.



Figure (20) Microphotographic showing the Sparry calcites occur as interparticle and intraparticle void-filling in intrasparite of Thitsipin limestone. (Under PPL)

CONCLUSIONS

The Pindaya Range is situated at the western part of the Southern Shan State. Most of the Lower Paleozoic rock units are well exposed in the Ye-gyan-zin village, about 7 km south of Pindaya Township. Generally the study area is rolling hilly terrain. Most of the topographic trends are nearly N-S direction. The western part is higher than the eastern. The eastern portion of the study area is sparse vegetation. Topographically four domains can be observed in the study area such as high lands, rolling lands, central low lands, lake and swampy area. Dendritic pattern is occurred in the

south eastern and centripetal pattern is common in the limestone region of western part.

There are four lithostratigraphic units in our study area and they are well exposed and widely distributed. They are Wunbye Formation (Middle Ordovician), Nan-on Formation (Late Ordovician), Linwe Formation (Early Silurian) and Plateau Limestone Group especially Thitsipin Formation (Early Permian). The Thitsipin limestone is composed of very thick bedded to massive, bluish grey limestone, rugose and tabulae coral bearing micritic and arenaceous limestone, dolomitic limestone, lithographic limestone, calcitic limestone and brecciated limestone which is exposed at highly mountain and karst topography. Fossils were found in the study area are Brachiopods, Crinoids, Gastropods, Bryozoan, *Favosities sp.* and some coral such as *Ipciphyllum sp.*, *Wentzellophyllum*, *Syringopora*, *Thomasiphyllum sp.*, and *Iranophyllum*. According to Folk's classification the carbonate rock units of the Plateau Limestone Group are biosparites, pelsparite, pelmicrite, intrasparite and dolostone. The Thitsipin limestones were deposited under the shallow warm marine environment because it is carbonate environment and their content of coral. The Plateau Limestone Group especially the Thitsipin Formation which is overlying unconformable upon older formations. The overall structure of the study area is characterized by longitudinal faults, cross faults and major Pindaya anticline in the study area. Mineralization is limited occurrences of barite. Brecciated limestone, calcitic limestone and red conglomerates can be used as road constructions raw materials.

ACKNOWLEDGEMENT

We are deeply grateful to Dr Khin Maung Hla, Professor and Head of Geology Department, Bago University for permission to carry out the present research paper. We are special thankful to Dr Tin May Tun, Professor of Geology Department, Bago University for her advice and comment on the study work. We are also grateful to Ko Thu Wun Thar and Ko Kaung Khant Zaw (MSc students) Department of Geology, Dagon University for their closely in valuable support and encouragement throughout the field investigation. My special thanks go to Professor Dr Kyi Chan Nyein, Head of English Department, Bago University for reading the manuscripts. Finally, We wish to thank the Department of Higher Education for financial support.

REFERENCES

- [1] Aye Ko Aung, 2002. Guide to the stratigraphy of the Ye-U, Linwe, Thitsipin and Nwabangyi Areas, Ywa-ngan Township, Southern Shan State, Myanmar.
- [2] Aye Ko Aung, 2002, Atlas of the Paleozoic Fossils from Shan State, Myanmar. Department of Geology, Dagon University: 33p.
- [3] Brown, I.C and Sondhi, V.P, 1933. The geology of the country between Kalaw and Taunggyi, Southern Shan State. *Rec.Geol. Survey India*, V.67, PP.166, 247 V.P-1933.
- [4] Bander, F., 1989. Geology of Burma. *Gebuder Borntraeger, Berlin, Stuttgart*, 278 p.
- [5] Garson, M.S, Amos, B.I and Mitchell, A.H.G, 1976. The geology of The area Around Nyaunga and Ywa-ngan. Southern Shan State, *Burmer Overseas Mem. Inst. Geology Sic.* No. 2. PP 1-77.
- [6] Myint Lwin Thein 1973, The lower Paleozoic stratigraphy of western part of the Southern Shan State, Burma Geol. Soc, Malaysia, Bull.6, 143-163.
- [7] Ma Than Sein, 1994, Geology and sedimentology of the Yeganzin Area. Pindaya Township, MSc Thesis, Department of Geology University of Yangon (unpublish).
- [8] Reed, F, R, C., 1936. The Lower Paleozoic faunas of the southern Shan State. *Palaeont. India, new series*, 21(3); 130p.
- [9] Wolfart et al., 1984. Stratigraphy of the western Shan Massif, Burma. *Geologieshes Jahrbuch*, Heft 57, Hannover, 3-9

Clay Mineral Identification of the Natma Formation of the Theingon Area, Mingin Township, Sagaing Region

Yee Myo Oo⁽¹⁾, Me Me Aung⁽²⁾

⁽¹⁾Yadanabon University, Myanmar

⁽²⁾Myitkyina University, Myanmar

Email: yeemyoo511@gmail.com

ABSTRACT

This paper presents the clay mineral identification of the Natma Formation of the Theingon area. The Theingon area is situated in Mingin Township, Sagaing Region. It belongs to the south-western margin of the Chindwin Basin. This paper intend to chemistry of mudrock and their disadvantage. For ground water and oil and gas resources clay layer is essential capped and based layer due to its impervious nature. To construct highway road and buildings, we must avoid or excavate clay layers because of its impervious nature and swelling and shrinking effects. According to the result, if we construct highway roads and buildings we must be known the effects of clay minerals. This paper intends to support engineering work by knowing the properties of clay minerals. If we know properties of clay minerals, we can easily solve soil problem about it.

KEYWORDS: *clay mineral, mudrock, impervious, swelling, shrinking*

1. INTRODUCTION

The Theingon area is situated in Mingin Township, Sagaing Region (Fig. 1). It lies between Latitude 22°52'N to 23°0'N and Longitude 94°13'E to 94°30'E of one-inch topographic maps 84-J/1 and 84-J/5. The Theingon area is situated at the south-western margin of the Chindwin Basin.

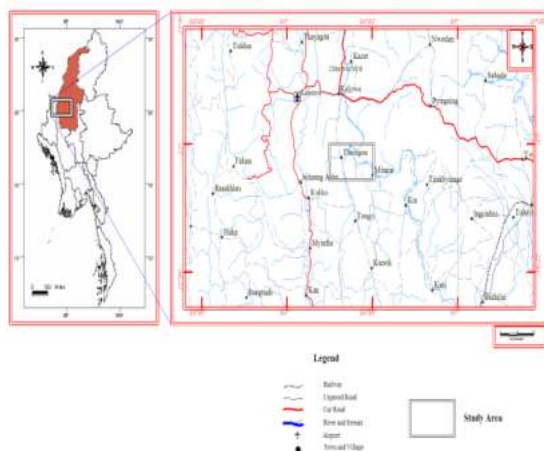


Fig. (1) Location map of the Theingon area

The references are cited as follows;

-Aung Khin and Kyaw Win (1969)

-Aye Lwin (1993)

-Lawmsanga (1982)

2. STRATIGRAPHY

2.1 General Statement

The Theingon area is mainly composed of the Pondaung Formation (Middle-Late Eocene), the Yaw Formation (Late Eocene), the Letkat Formation (Early-Middle Miocene), the Natma Formation (Middle-Late Miocene), the Shwethamin Formation (Late Miocene), Irrawaddy Formation (Late Miocene-Pliocene), and Mingin Gravels (Pleistocene). This paper presents the clay mineral identification of the Natma Formation of the study area. This paper intends to support engineering work by knowing the properties of clay minerals. If we know properties of clay minerals, we can easily solve soil problem about it.

2.1.1 Natma Formation

The Natma Formation is composed of clay, shale with interbedded sandstones and silty clays. Clays are yellowish to reddish brown, fairly hard, massive and silty (Fig. 2, 3).



Fig. (2) Massive and silty clays of the Natma Formation (Moktha Chung, Lat. 22°57' N, Long. 94°18'30" E)

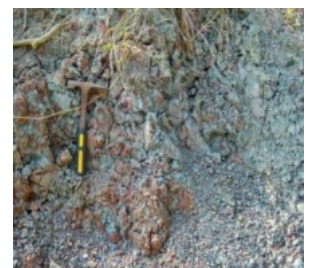


Fig. (3) Mottled and variegated clays of the Natma Formation (Lat. 22°58' N, Long. 94°18' E)



Fig. (4) Geological map of the Theingon area

Geology by Yee Myo Oo, 2012

3. EXPERIMENT

3.1 Experiment apparatus

The dried samples were analysed by XRD technique. This experiment is carried out by Universities' Research Center (URC), Yangon.

3.2 Sample Preparation and Method of Study

For clay mineral analysis, various soil samples were collected along the Moktha Chaung section (Lat. 22°57' N and Long. 94°18' E) of the Natma Formation of the Theingon area. Totally, nine samples were collected to analysis. Before analysis, these samples are required to separate from other non clay minerals and cementing materials. Firstly, the sample is mixed with water in a beaker and stirring with a glass rod, and then stand for a few minutes. Secondly, the suspension clay minerals are transferred into another beaker and then the beaker is stand until all the clays are settled down. The usual size fraction separated for clay mineral analysis is < 2 μ m. Finally, the settled clay particles are placed on a filter paper and in a good ventilation place.

4. CLAY MINERAL ANALYSIS

4.1 General Statement

Clay is very important material in geotechnical engineering, because it is often observed in geotechnical engineering practice. Generally this soil type has numerous problems due to its low strength, high compressibility and high level of volumetric changes. Clay minerals are very electrochemically active; thus, they affect soil microstructures. Due to these characteristics, many important soil problems related to clay have been observed in the past, the importance of which is understood. X-ray diffraction (XRD) provides the most efficient method for the determination of clay minerals in mudrocks, sandstones and limestones.

4.2 Interpretation of XRD Spectra of Clay Minerals

Under these analyses, samples N-1 to N-3 series. L-1 to L-3 series and Y-1 to Y-3 series represent the clay samples from Natma Formation. From XRD spectrum, the constituent clay minerals and other associated minerals can be interpreted as follows.

For N-1 to N-3

In XRD spectrum, the two theta values of N-1 are identical with 86-1561> Quartz and 89-0950> Magnetite files. So, N-1 contains quartz and magnetite minerals. According to XRD data, two theta values of N-2 are identical with 85-0865> Quartz, 52-1044> Chlorite-serpentine, 22-0712> Nimite and 73-0603> Hematite files (Brindley, 1953). So, this sample contains quartz, chlorite, serpentine, nimite and hematite minerals. The XRD data of N-3 are identical with 85-0865> Quartz, 52-1044> Chlorite-serpentine, 73-0603> Hematite and 71-0071> Pyrolusite files. So, N-3 contains quartz, chlorite, serpentine, hematite and pyrolusite minerals.

For Y-1 to Y-3

In XRD spectrum, the two theta values of Y-1 are identical with 85-0794> Quartz, 24-0506> Clinocllore and 75-0938> Kaolinite files. So, Y-1 contains quartz, clinocllore and kaolinite. In XRD study, the two theta values of Y-2 are identical with 85-0865> Quartz, 52-1044> Chlorite-serpentine files. So, this sample contains quartz and chlorite minerals. In XRD spectrum, the two theta values of Y-3 are identical with 86-1561> Quartz, 73-0603> Hematite, 89-6538> Kaolinite and 29-0701> Clinocllore files. So, Y-3 contains quartz, hematite, kaolinite and clinocllore minerals.

For L-1 to L-2

In XRD study, the two theta values of L-1 are identical with 86-1561> Quartz and 06-0263> Muscovite- 2M1 and 73-1415> Amesite files. So, L-1 contains quartz, muscovite and amesite. The XRD data of L-2 are identical with 86-1561> Quartz, 52-1044> Chlorite-serpentine and 29-0701> Clinocllore files. So, this sample contains quartz, chlorite and clinocllore minerals. The XRD data of L-3 are identical with 82-0511> Quartz, 49- 1409> Muscovite- 2M1, 52-1571> Amesite and 10-0393> Albite files. So, this sample contains quartz, muscovite, amesite and albite minerals.

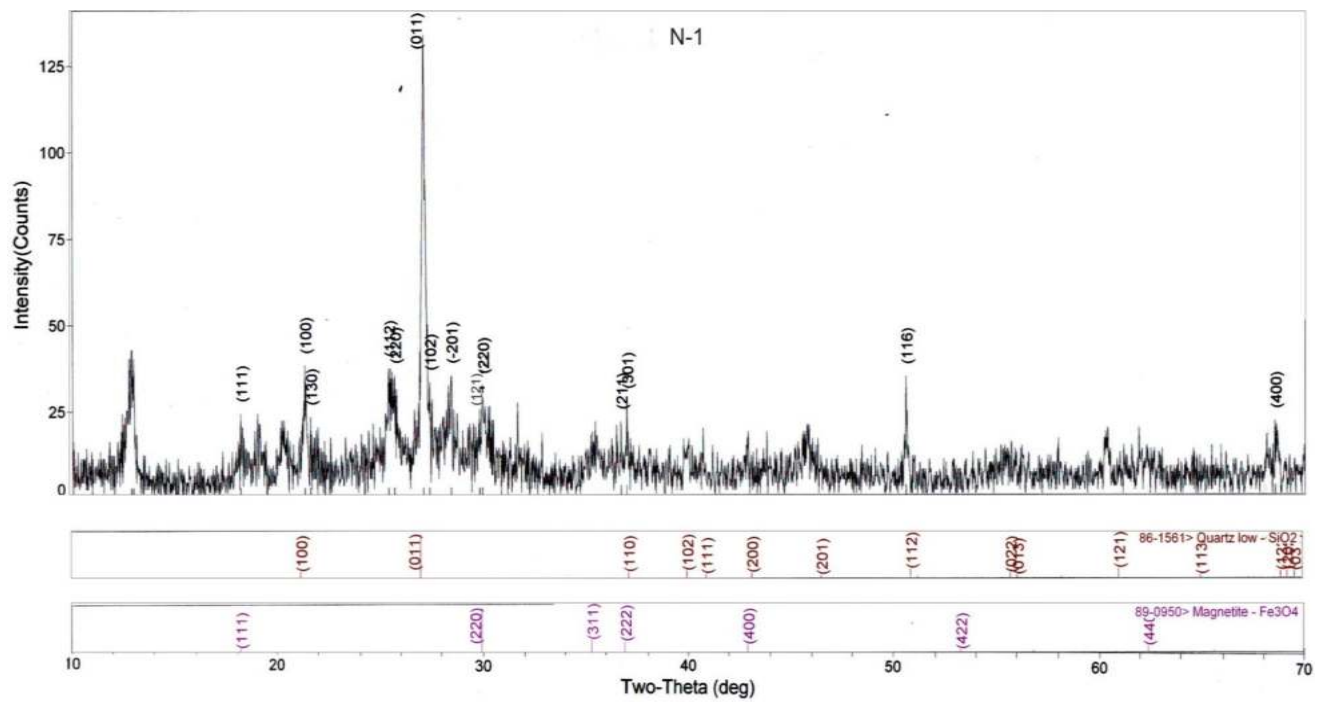


Fig. (5) XRD Spectrum of N-1

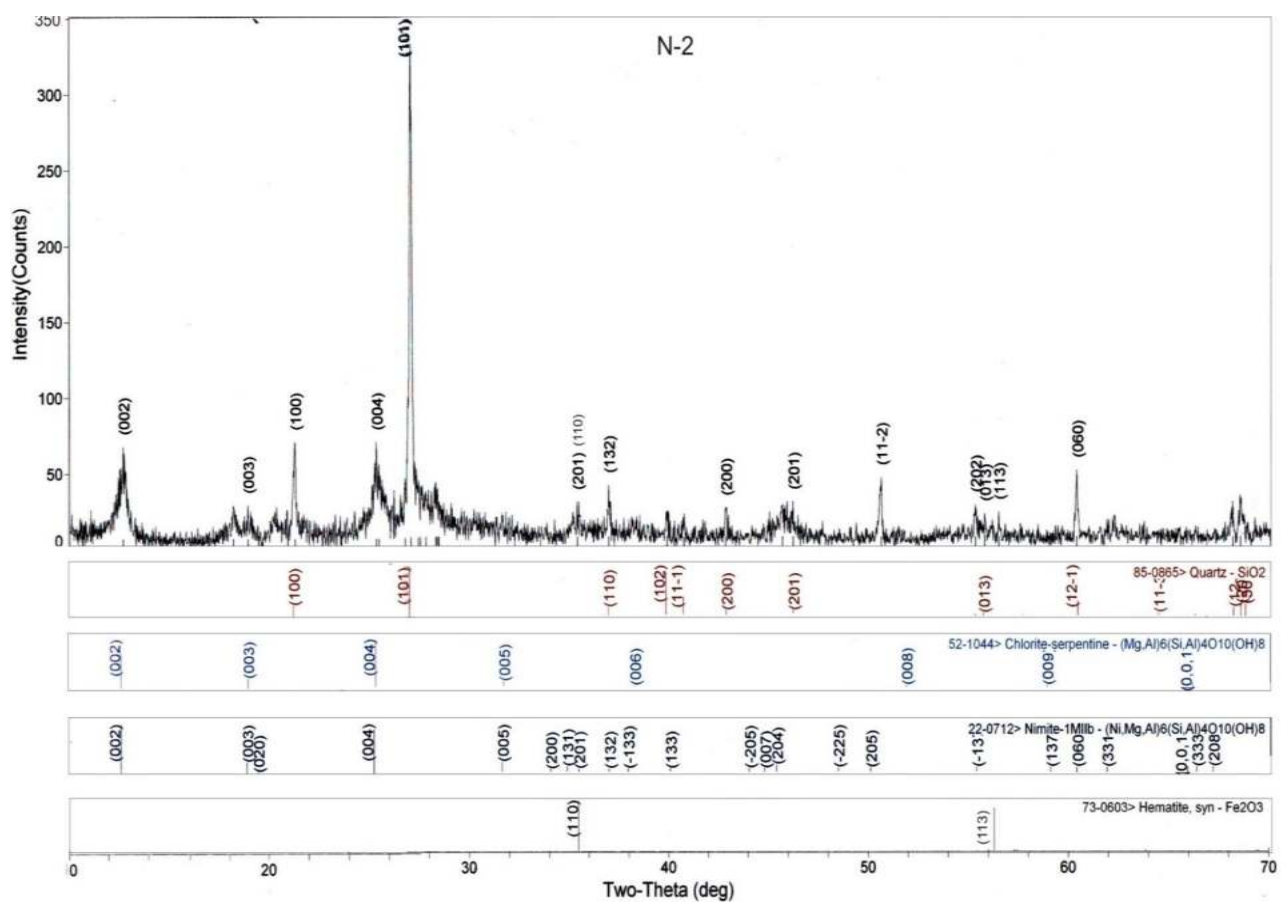


Fig. (6) XRD Spectrum of N-2

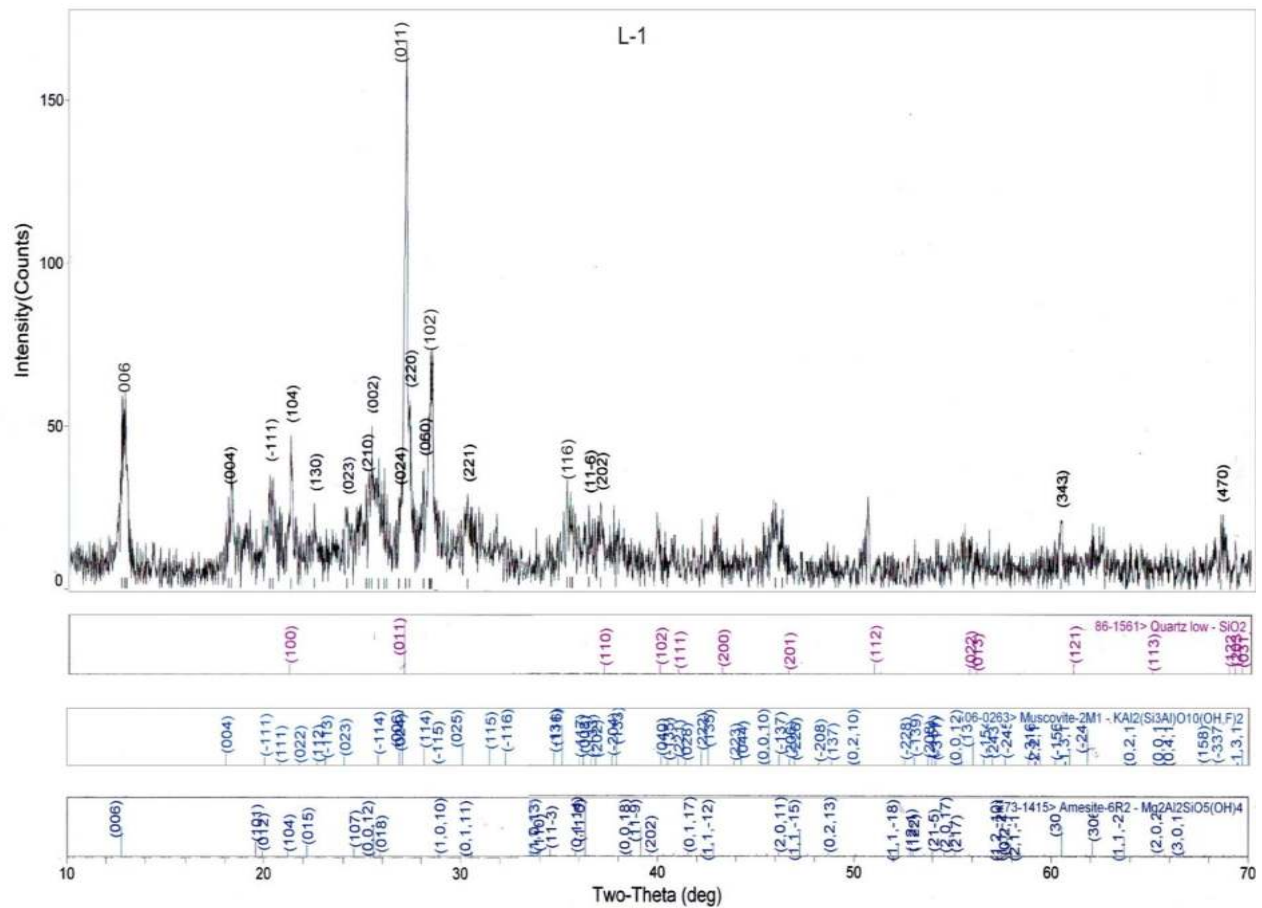


Fig. (7) XRD Spectrum of N-3

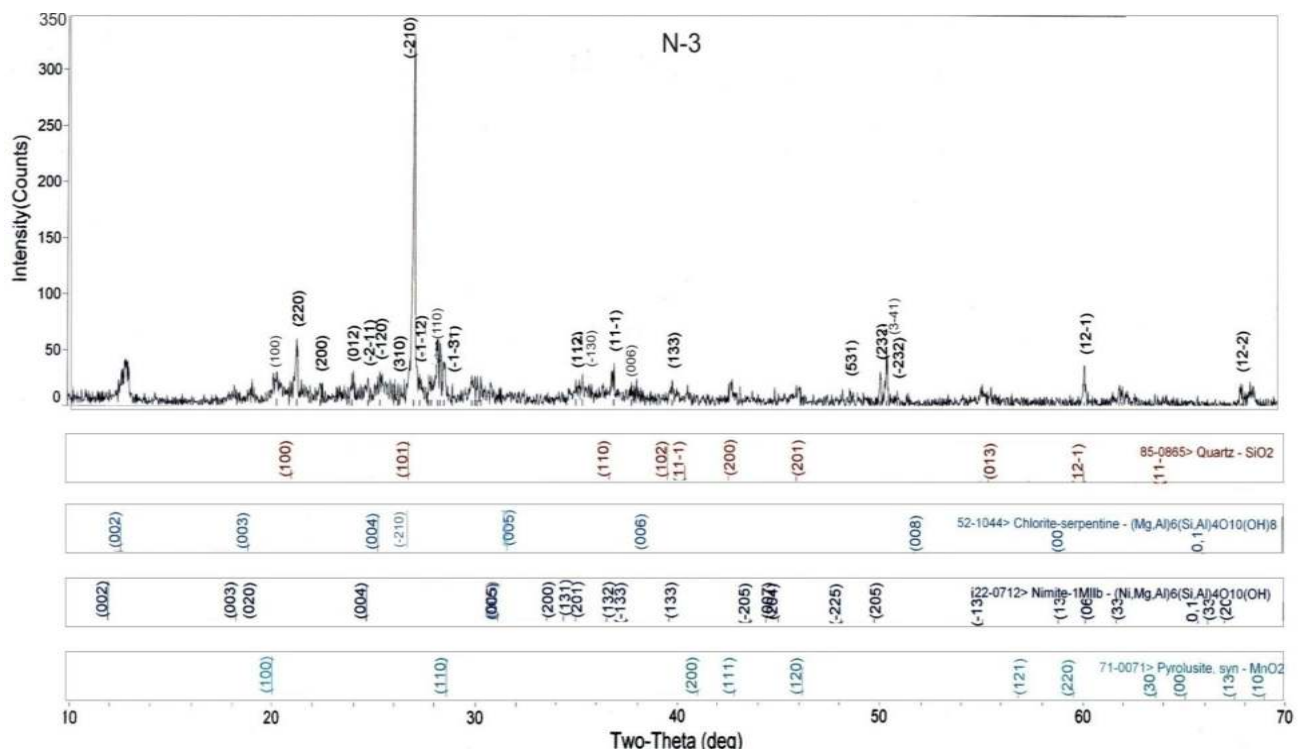
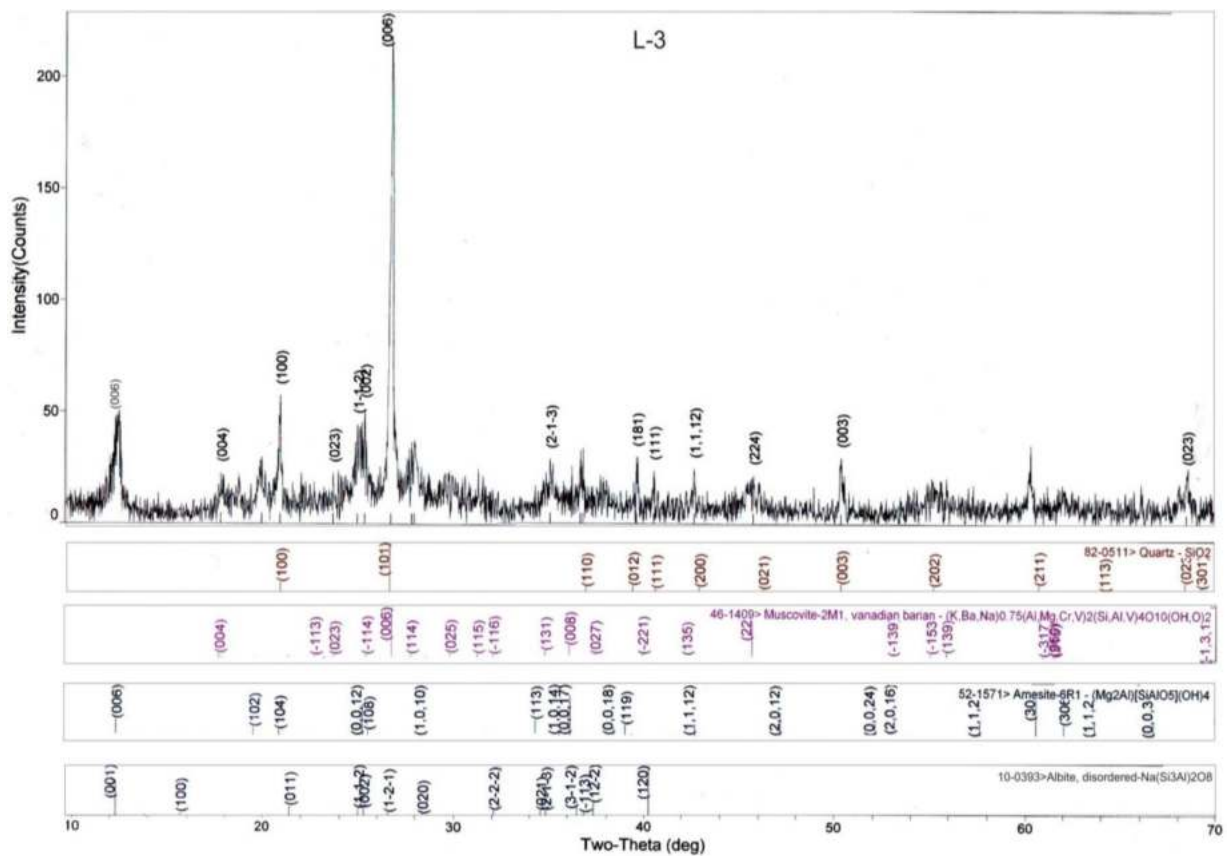
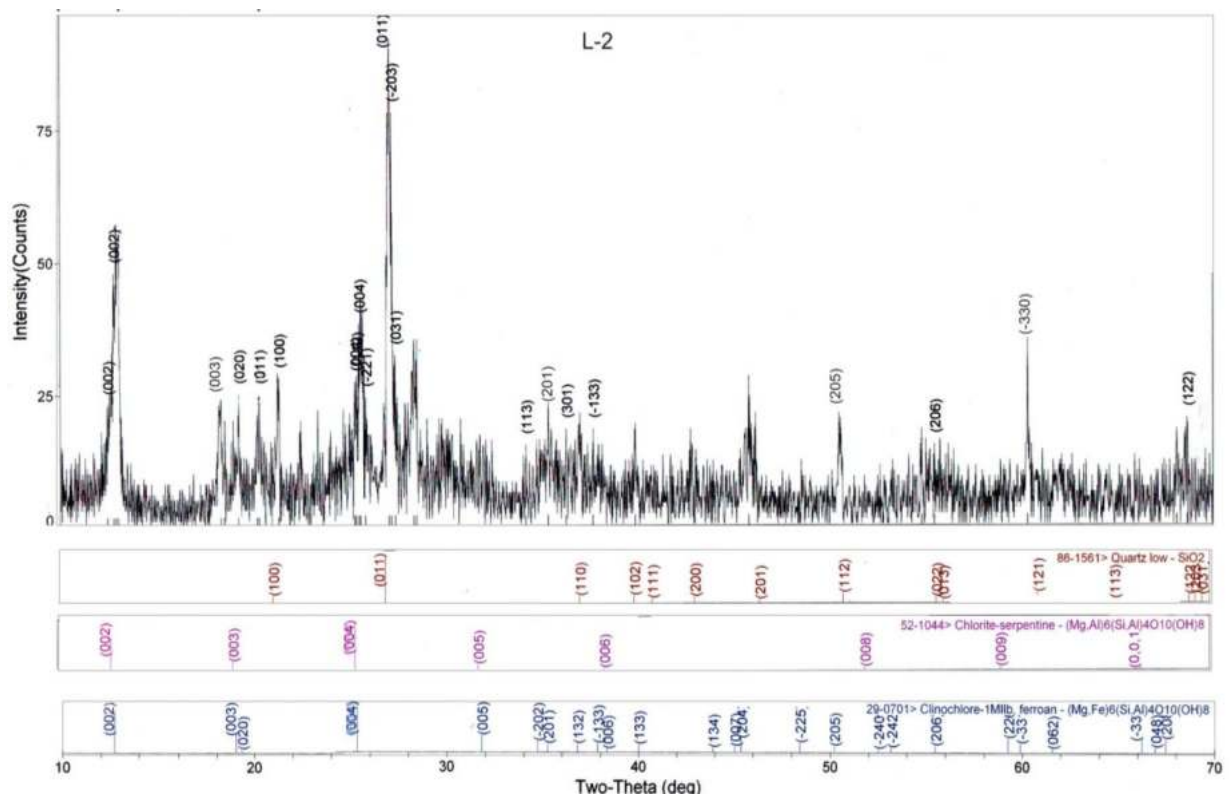


Fig. (8) XRD Spectrum of L-1



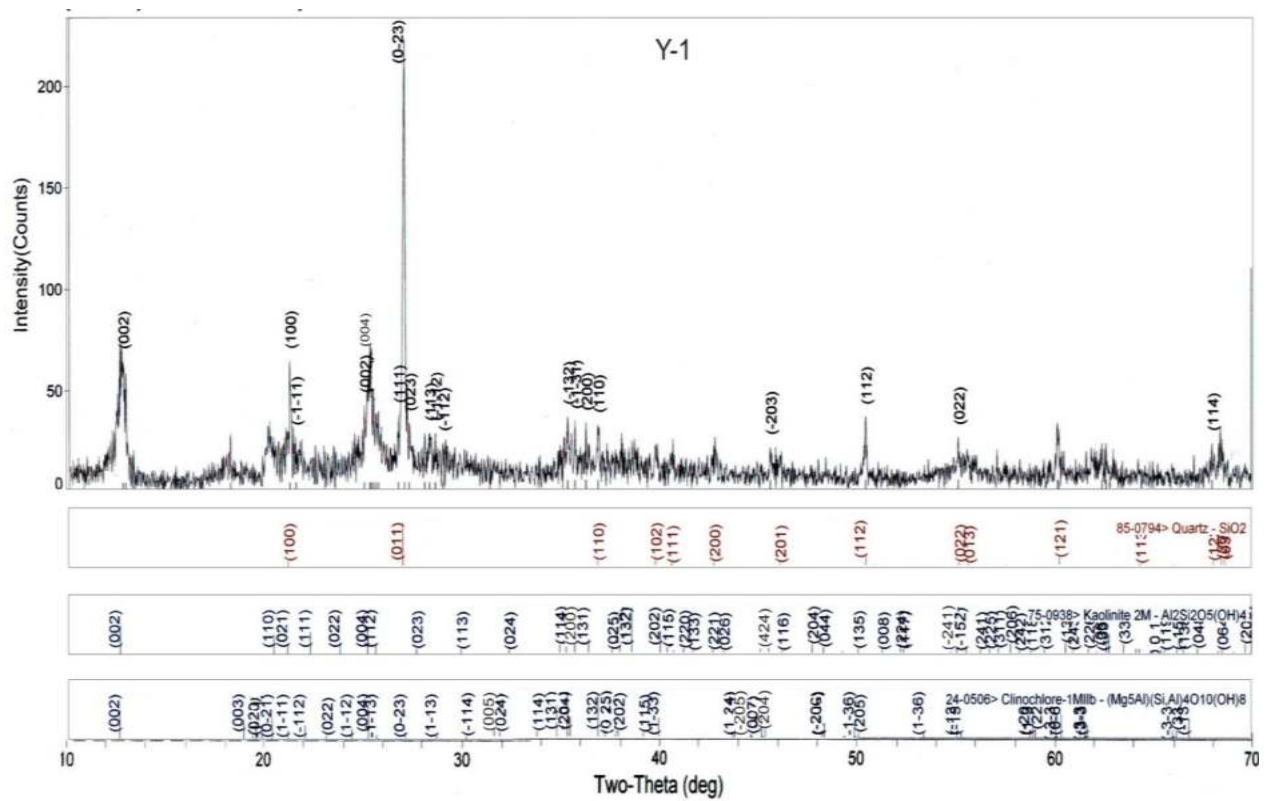


Fig. (11) XRD Spectrum of Y-1

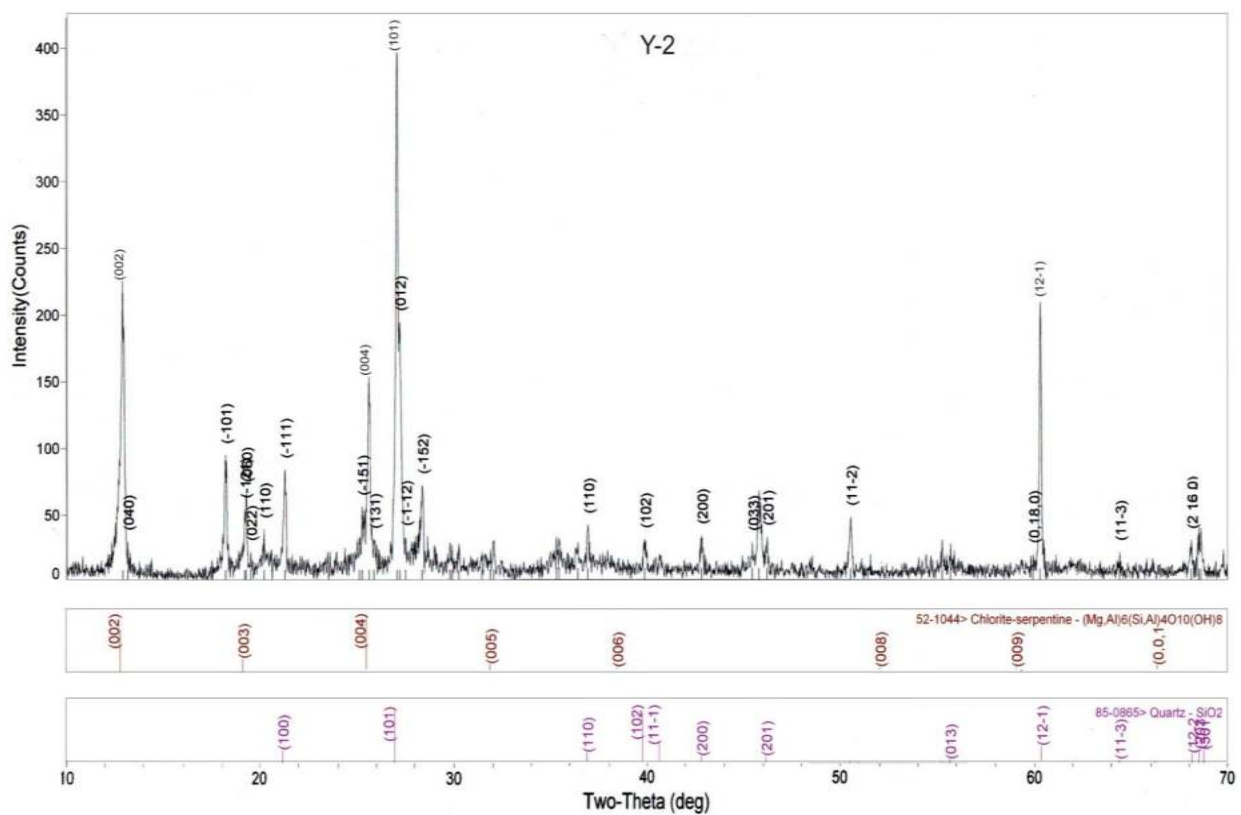


Fig. (12) XRD Spectrum of Y-2

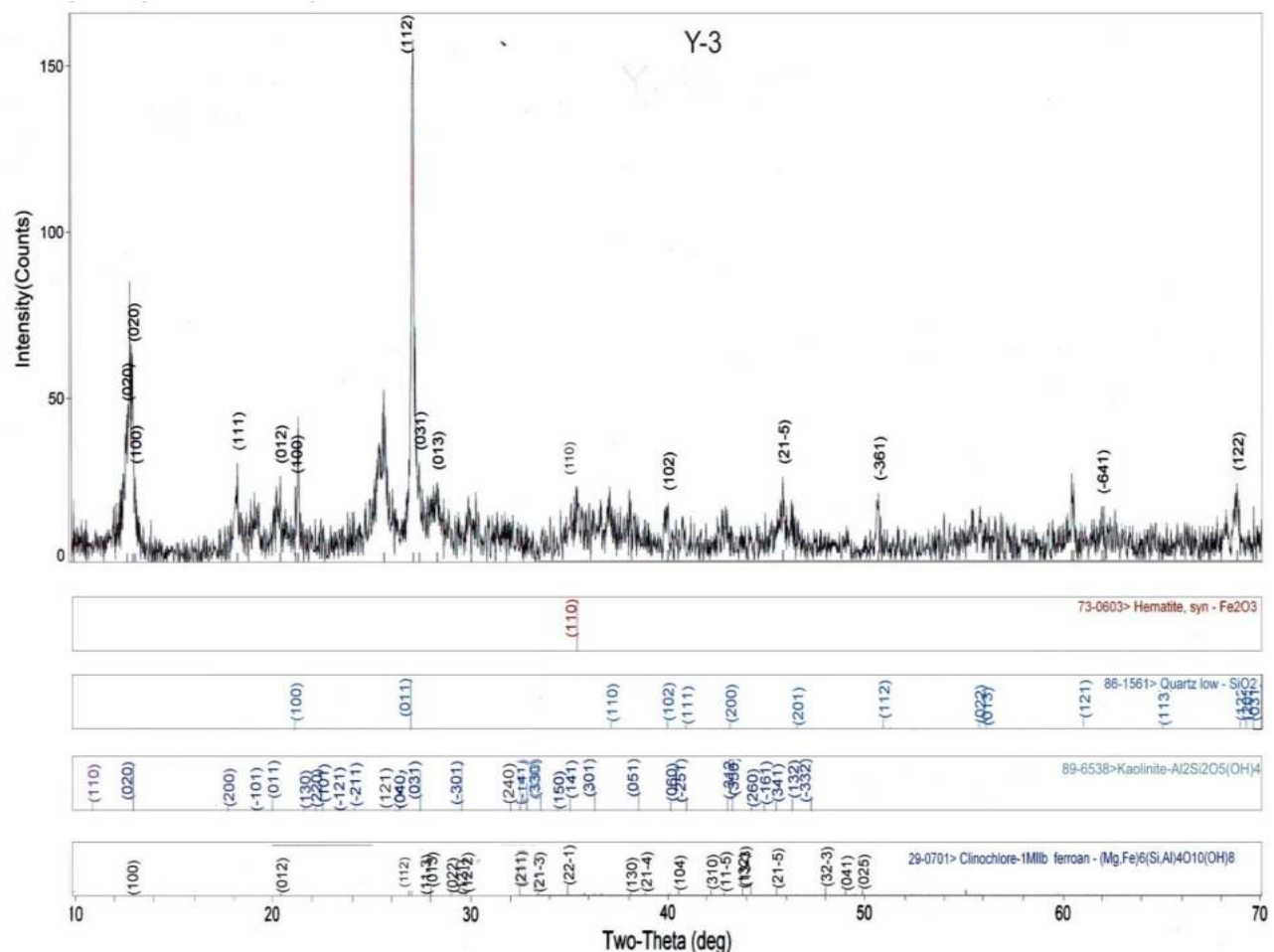


Fig. (13) XRD Spectrum of Y-3

4. CONCLUSIONS

From the result of X-ray diffraction (XRD) technique, the soils of the Theingon area soils have a high content of clay minerals. The main types of clay minerals in the study area are chlorite, kaolinite and muscovite and other associated minerals such as quartz, serpentine, hematite, albite, magnetite and pyrolusite are present. Amesite, clinocllore and nimite minerals are the members of chlorite group (Kunze, et al., 1953). Chlorite may be more abundant in clays deposited in brackish and fresh-water environment than in those deposited under open marine conditions (Pettijohn, 1987). Chlorite also develops at depth, and into the zone of incipient metamorphism (Tucker, 1988). Kaolinite is dominant in low latitude area, particularly off major rivers draining regions of tropical weathering, and illite and chlorite are more common in higher latitude marine muds (Pellant, 1992). The illite (or the clay-mica) group is basically a hydrated microscopic muscovite. Illite is the most abundant and consists of a family of fine-grained micaceous minerals (Fairbridge, 1987).

Monywa-Yagyi-Kalewa car road passes along the Natma Formation of the Theingon area. Many soils have a high content of clay minerals, some of which can act

like sponges and absorb large quantities of water, causing the clay mineral to increase substantially in volume. These soils are expansive soils. The Natma Formation is composed mainly of expansive soils which have high content of clay minerals. Damage to structures is commonly related to soil characteristics, with expansive (shrink/swell) soils and collapsing soils causing the most problems. The expansive soil will be swelling upon wetting and shrinking to drying. This behavior can damage of construction structures, particularly, light buildings and roads. The best means of preventing or reducing damage from expansive soils is to avoid them. However, when no other choice is possible except to place a structure on a potentially expensive soil, engineering procedures such as removal of the soil, application of heavy loads, preventing access of water, prewetting and stabilization are necessary. Therefore, to construct highway road in this area, we must excavate clay layers.

ACKNOWLEDGEMENT

I would like to express my thanks to Dr Aung Aung Min, Rector of Yadanabon University, for his permission to carry out this paper. I greatly acknowledge to Ethical Research Committee, Internal Review Committee and

External Review Committee of TULSOJRI. I wish to express my gratitude to Dr. Si Si Khin and Dr. Tint Moe Thuza, Pro-Rectors for providing all departmental facilities. I am greatly indebted to Professor Dr. Htay Win, Geology Department, Yadanabon University, for his encouragement and permission to perform this research paper. I sincerely express my gratitude to Dr. Khaing Khaing San, Professor of Geology Department, Yadanabon University for her advice and suggestion. Special thanks are also due to all local people of Theingon Village for their valuable helps and facilities throughout the field work.

REFERENCES

- Aung Khin and Kyaw Win,. Geology and Hydrocarbon Prospect of the Burma Tertiary Geosyncline. *Journal. Union of Burma, Sci. Tech.*,2, 1969.
- Aye Lwin, *Sedimentology of the Sandstones of the Mahudaung Area, Kani and Mingin Townships*, M.Sc Thesis, University of Mandalay, unpublished, 1993.
- G.W, Brindley, *Identification of Clay Minerals by X-Ray Diffraction Analysis*. Pennsylvania State University, Pennaylvania, 1953.
- R.W, Fairbridge, J, Bourgeois, *The Encyclopedia of Sedimentology*, Dowden Hutchinson and Ross, Inc, 1978.
- G.W, Kunze, E.H, Templin, J.B, Page, *The Clay Mineral Composition of Representative Soils from Five Geological Regions of Texas*. Agricultural and Mechanical College of Texas, 1953.
- Lawmsanga, *Stratigraphy and petrology of the sedimentary Rocks in the Kyigon- Kalewa Area*, M.Sc Thesis, University of Mandalay, unpublished,1982.
- C, Pellant, *Rocks and Minerals*. Landon, New York, 1992.
- F.J, Pettijohn, *Sedimentary Rocks*. 3rd edition. Harper and Raw Press, New York, 1987.
- L.A, Raymond, *Petrology: the Study of Igneous, Sedimentary and Metamorphic Rocks*. Appalachian State, University, 1993.
- M.E, Tucker, *Techniques in Sedimentology*. Blackwell Science, 1988.
- C.E, Weaver, *A Discussion on the Origin of Clay Minerals in Sedimentary Rocks*. Shell Oil Company, Houston, Texas, 1941.

Detection of Land Use and Land Cover Changes Before and After Shwegyin Dam Construction

Ei Mon Mon Kyaw ⁽¹⁾, Su Su Hlaing ⁽²⁾, Shwe War ⁽³⁾

⁽¹⁾ Department of Civil Engineering, Technological University (Thanlyin), Myanmar

⁽²⁾ Department of Civil Engineering, Technological University (Thanlyin), Myanmar

⁽³⁾ Department of Civil Engineering, Technological University (Thanlyin), Myanmar

eimonmon1110@gmail.com
susuhlaing.26civil@gmail.com
shwewartutgi@gmail.com

ABSTRACT: The continuous investigating of land use and land cover changes information plays an important factor in a sustainable development of any region. This study aims to investigate the land use and land cover changes in Shwegyin River Basin before and after constructing Shwegyin dam. A pixel based supervised classification - maximum likelihood algorithms was applied to two temporal Landsat imageries, Landsat 5 TM for 2000 and Landsat 8 OLI for 2020 to detect land use and land cover changes observed in Shwegyin River Basin. ArcGIS 10.5 and ENVI 4.2 software were used to detect land use and land cover changes in this study. The river basin was classified into five land use classes: water bodies, forest, urban and built-up land, agricultural land and bare land. According to the results, almost 80% of the river basin was covered with forest. After constructing Shwegyin dam, the amount of water surface area gradually increased meanwhile the forest and agricultural areas decreased respectively. Urbanization was developed, however, the bare land was decreased in the river basin. For land use and land cover maps of 2000 and 2020, accuracy assessment is 78% and 86% and kappa coefficient is 0.73 and 0.81 respectively. The presented results will be valuable for watershed management and land use planning activities in the future.

KEYWORDS: *ENVI, Arc GIS, land use and land cover, supervised classification, change detection*

1. INTRODUCTION

Land cover is the physical characteristics of the earth's surface, whereas land use is the various human activities of land cover. The land cover and land use change is caused by both natural and anthropogenic factors. Therefore, a typical watershed that includes multiple forms of land uses/land covers (LULC) might influence the hydrological characteristics of watersheds. Generally, land cover refers to the physical land type such as how much of a region is covered by forests, impervious surfaces, agricultural lands, wetlands and open water, whereas land use documents how people are using the land for development, conservation or mixed uses [3]. Land use and land cover change (LULCC) assessment helps to detect the extent of human influence on natural environment.

Nowadays, the most prominent methods are remote sensing techniques for Land Use/Land Cover change

analysis. Multi-temporal remote sensing (RS) based on change detection analysis has repeatedly been used in different aspects of land cover change [12]. RS platforms continuously capture the Earth's surface and decision makers can easily apply satellite imagery to monitor dynamics of change. LULC change analysis using RS techniques gives an opportunity to obtain results with low costs, less time consumption and good accuracy, and geographical information systems (GIS) allow updating results whenever new data is available [9]. Utilization of open source data is a good choice to improve the skills in RS and GIS tools, in particular for scientists from less-developed countries. In this context, Landsat satellite images are frequently used for LULC change detection analysis. With RS data, different change detection algorithms are available and repeatedly applied, such as principal component analysis, fuzzy classification, and post classification methods [11].

The main objective of the current study was (1) to apply open source datasets of Landsat for LULC change detection, (2) to classify and analyze the land use and land cover changes using RS and GIS techniques for Shwegyin River Basin.

2. STUDY AREA

This study is the detection of land use and land cover changes in Shwegyin River Basin. Shwegyin River Basin is one of the sub basins of Sittaung River Basin. Shwegyin River is the tributary of the Sittaung River which is the one of four major rivers such as Ayeyarwaddy, Sittaung, Thanlwin and Chindwin rivers in Myanmar. Shwegyin River Basin lies between (longitude 96°45' and 97°10' East) and (latitude 17°30' and 18°30' North) and is located in Bago Region, Myanmar. The high mountains are formed in the northern and eastern part and plain areas are in the western and southern part of the basin. The highest and lowest elevation are 1883 m and 5 m above mean sea level.

The Shwegyin River Basin was delineated by locating outlet point at latitude 17°55' N and longitude 96°52' E. So, the catchment area of Shwegyin River Basin is about 1728 km² and the climate in it is tropical. There is significant rainfall in most month of year. The average annual rainfall in Shwegyin River Basin is about 3600 mm. According to collected rainfall data, the annual maximum and minimum rainfall are 4100 mm and 2800 mm. The average annual maximum and

minimum temperature are 33°C and 22°C. Shwegyin River Basin has a meteorological and hydrological station, which is situated in the mouth of the Shwegyin River.

In Shwegyin River Basin, there is only one hydropower dam which is called Shwegyin dam. Shwegyin dam is located at 17°58'15.6" north latitude and 96°56'9.79" east longitude and is situated near Kyauknaga village, about 6.0 miles northeast from the Shwegyin town. The catchment area in the upstream of Shwegyin dam is about 878 km². This dam is crossed the Shwegyin River. The construction of Shwegyin dam began in 2002, the first generator was operational in December 2010 and it was formally opened in 2011. This dam is embankment, rock-fill type. The install capacity of Shwegyin dam is 75 MW and annual generation is 262 GWh. The purpose of dam is only for the use of hydroelectric power generation.

The catchment area of Shwegyin River Basin is shown in figure 1.

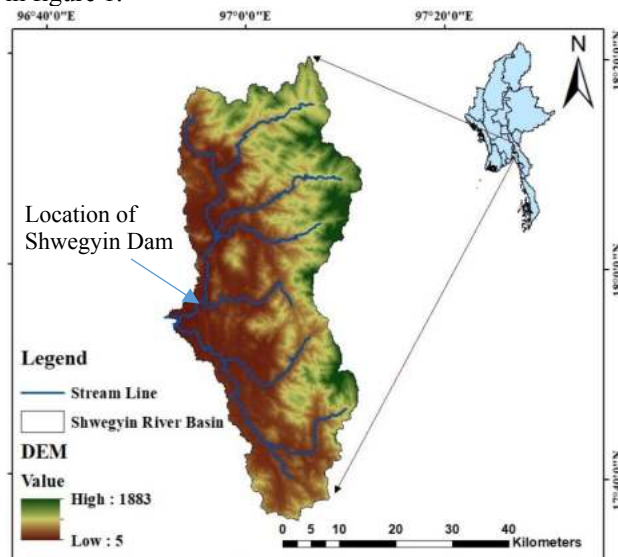


Figure 1. Study Area of Shwegyin River Basin

3. DATA COLLECTION

For the current study, land use and land cover changes detection during two decades which is between 10 years before Shwegyin dam and 10 years after Shwegyin dam are to be analyzed. So, period of 2000 before dam and 2020 after dam were considered. This study is based on analysis of satellite imageries. In this study, multi-temporal Landsat images had been applied. Landsat 5 TM (thematic mapper) data for the period of 2000 and Landsat 8 OLI (Operational Land Images) data for the period of 2020, path/row of 132/47 and 132/48 were used. The spatial resolution of both imageries are 30 m. These Landsat imageries were acquired free from USGS (United States of Geological Survey) Earth Explorer website for generating land use/land cover maps. The details of satellite data are shown in Table.1

The secondary data such as Digital Elevation Model (DEM) and topographic map were acquired from different sources. DEM was obtained from USGS (United States of Geological Survey) Earth Explorer website with 30 m spatial resolution. It was used for delineating watershed. Topographic map was

downloaded from MIMU (Myanmar Information Management Unit) data sets.

Table 1. Landsat TM 2000 and Landsat OLI 2020 imageries metadata

Satellite Sensor	Scene Date	Path/Row	Spatial Resolution (m)
Landsat 5 TM	12 Feb-2000	132/47	30
		132/48	
Landsat 8 OLI	23 Jan-2020	132/47	
		132/48	

4. MATERIALS AND METHODS

To detect land use and land cover changes before and after construction of Shwegyin dam in Shwegyin River Basin, the following processes were taken step by step.

4.1 Watershed Delineation

Watershed delineation means identifying boundaries that represents the contributing area for a control point or outlet. Digital Elevation Model (DEM) was used as input for delineating watershed. Watershed was delineated by using Arc GIS software. Firstly, DEM was downloaded from United State of Geological Survey (USGS) Earth Explorer website. And the next step was to create a fill to remove any sinks in the digital elevation model (DEM) and create a flow direction. Then, flow accumulation was calculated and outlet point was identified. After finishing above steps, watershed delineation was generated.

4.2 Image Processing and Classification

In this study, ENVI software version 4.2 was used to detect land use and land cover changes. Firstly, layer stacking of the two images (Path 132 - Row 47 and 48) and subsetting or extracting the images based on the polygon of the study area was done as the image preprocessing step.

And then, five classes for the images were identified. These are water bodies, forest, urban and built up land, agricultural land and bare land. Maximum likelihood approach was applied for classification stage to generate the thematic map of land use/land cover and to analyze the changes that occurred from 2000 to 2020. There are more than 20 training sites or ground truth points collected for each class. Description of land use and land cover classes are shown in table 2.

Table 2. Description of Land use and Land cover classes.

Code	Class Name	Description
1	Water Bodies	This class describes the land covered with water either along the river, stream, lake, pond and

Table 2. Continued

Code	Class Name	Description
1	Reservoir	It can be fresh and salt water.
2	Forest	This describes the areas with evergreen trees. It can be dense and mixed forested area.
3	Urban and Built up Land	This class describes the areas covered with buildings in the rural and urban settlement. It includes concrete structure such as commercial, residential, industrial, transportation and other uses
4	Agricultural Land	This class describes the land used for growing farms, vegetation, plantation and crop. It can be divided into fallow field and crop field.
5	Bare Land	This describes the land that is not covered by vegetation and uncultivated agricultural lands. This result from abandoned crop land, eroded land due to land degradation and weathered road surface.

4.3 Accuracy Assessment

For post classification, accuracy assessment is a crucial part of studying image classification and thus land use and land cover changes detection in order to understand and estimate the changes accurately. Accuracy assessment is the comparison of a classification with ground-truth data. This assessment was carried out using an error matrix. In this study, accuracy assessment was done for the Landsat 5 TM and Landsat 8 OLI satellite image using ground truth points. The reference data was prepared by considering random sample points from the topographic map and historical data of Google earth. There were 20 ground truth samples for each classes had been collected to use in the accuracy assessment.

5. RESULTS AND DISCUSSIONS

The results of the classification process for year 2000 (before construction dam) and 2020 (after construction dam) provide an overall estimate of land use and land cover distribution in the study area.

5.1 Land Use and Land Cover Classification

By using satellite images of Landsat 5 TM 2000 and Landsat 8 OLI 2020, five land use and land cover classes

were generated: water bodies, forest, urban and built up land, agricultural land and bare land. These land use and land cover have spatial pattern and subject to change over time. Here below the land use and land cover maps of Shwegyin River Basin in the period of 2000 and 2020 are represented by figure 2 and 3. Table 3 and 4 show the coverage area (km²) and (%) of land use and land cover in Shwegyin River Basin in Year 2000 (before construction of dam) and 2020 (after construction of dam). Figure 4 and 5 show the area amount of land use and land cover class in Shwegyin River Basin in Year 2000 and 2020.

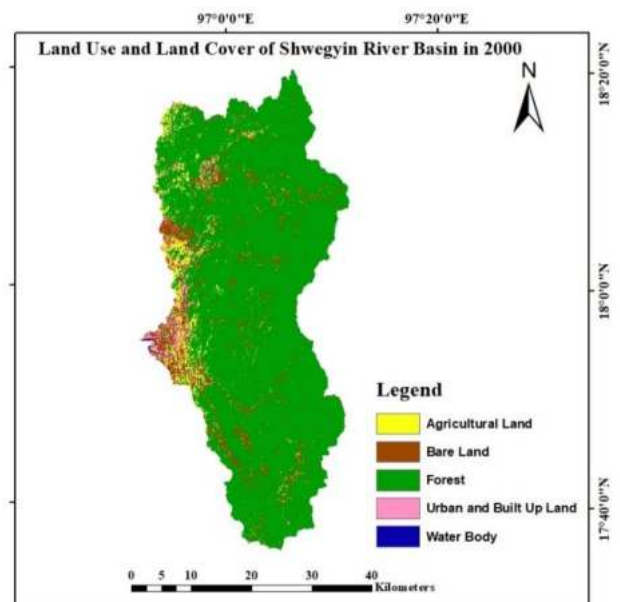


Figure 2. Land Use and Land Cover Map of Shwegyin River Basin in Year 2000

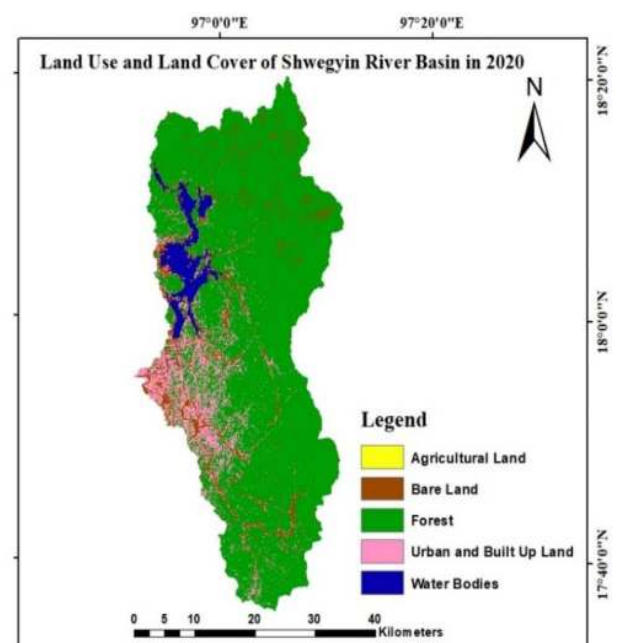


Figure 3. Land Use and Land Cover Map of Shwegyin River Basin in Year 2020

Table 3. Coverage Area (km²) of Land Use and Land Cover classes in Year 2000 and 2020.

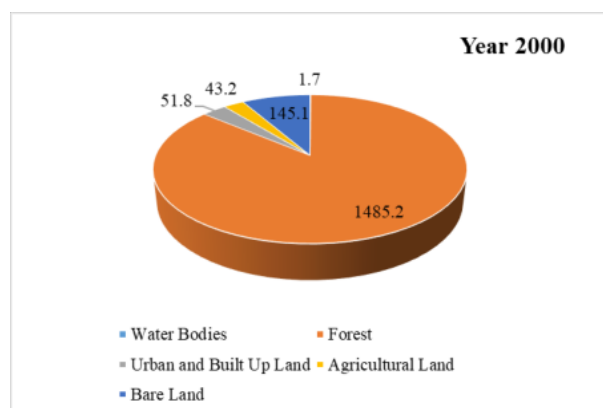
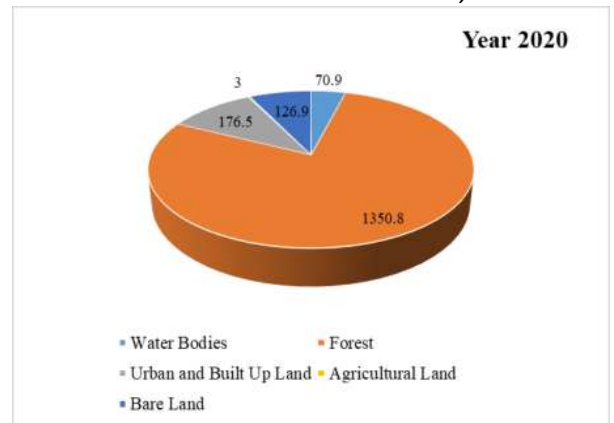
Land Use/ Land Cover Categories	Area (km ²)	
	2000 (Before Dam)	2020 (After Dam)
Water Bodies	1.7	70.9

Table 3. Continued

Land Use/ Land Cover Categories	Area (%)	
	2000 (Before Dam)	2020 (After Dam)
Forest	1485.2	1350.8
Urban and Built Up Land	51.8	176.5
Agricultural Land	43.2	3
Bare Land	145.1	126.9

Table 4. Coverage Area (%) of Land Use and Land Cover classes in Year 2000 and 2020

Land Use/ Land Cover Categories	Area (%)	
	2000 (Before Dam)	2020 (After Dam)
Water Bodies	0.1	4.1
Forest	86	78.2
Urban and Built Up Land	3.0	10.2
Agricultural Land	2.5	0.2
Bare Land	8.1	7.3

Figure 4. Area amount of Land Use and Land Cover (km²) in Shwegyin River Basin in Year 2000Figure 5. Area amount of Land Use/Land Cover (km²) in Shwegyin River Basin in Year 2020

5.2 Accuracy Assessment of Classification

Each of the land use/land cover maps was compared to the ground reference data to assess the accuracy of the classification. Over all classification accuracy for 2000, and 2020 are shown in table 5. According to results in table below, it is obvious that the accuracy assessment of Landsat TM images for 2000 is less than Landsat OLI for 2020. This can be due to the need of collecting more of reference samples and the low resolution of images on google earth pro to get better results.

Table 5. Accuracy Assessment and Kappa Coefficient of Land Use and Land Cover Class in Year 2000 and 2020

	2000 (Before Dam)	2020 (After Dam)
Overall Accuracy (%)	78	86
Kappa Coefficient (k)	0.73	0.81

5.3 Land Use and Land Cover Changes Before and After Construction of Shwegyin Dam

The amount of land use and land cover changes in Shwegyin River Basin between the period of 2000 and 2020 are shown in table 6. And, the changes of each classes of land use and land cover during two decades are explained below.

Table 6. Land Use and Land Cover Changes in Shwegyin River Basin from 2000 to 2020

Land Use/ Land Cover Categories	From 2000 to 2020	
	Area (km ²)	Area (%)
Water Bodies	+69.2	+4.0
Forest	-134.4	-7.8
Urban and Built Up Land	+124.7	+7.2
Agricultural Land	-40.2	-2.3
Bare Land	-18.2	-1.1

Source: Data was derived from Table 3 & 4

Note: positive (+) sign indicates rise up and negative (-) sign indicates fall down of magnitude of Land Use/Land Cover in different time frame.

1. Change in water bodies: Before constructing dam, the amount of water bodies was 1.7 km² (0.1% of Shwegyin River Basin) in the year 2000. The water bodies area in the Shwegyin River Basin was increased significantly after constructing Shwegyin dam and was 70.9 km² as well as 4.1% of the study area in the period of 2020.

2. Change in forest: Before Shwegyin dam, the area of forest for the year 2000 was approximately 1485 km², accounting for 86% of the total area. After constructing dam, the amount of forest area was gradually decreased to 1350.8 km² and 78% of Shwegyin River Basin in year 2020. The decrease in amount of forest during two decades was 134.4 km².

3. Change in urban and built up land: Urban and built up land in Shwegyin River Basin was significantly increased during two decades from 2000 to 2020. The amount of this land was 176.5 km², accounting for 10.2% of the total area in the year 2020. This class cover extent and its area percentage for the year 2000 was 3% of total basin area. It was occurred the change of built up land was increased to 7.2% from the period of 2000 to 2020.

4. Change in agricultural land: In Shwegyin River Basin, it was found that the area amount of agricultural land was less than other classes. Agricultural land was among the land use land cover types that showed decrease in area. The area of this class was 43.2 km² which is 2.5% of the area of Shwegyin River Basin in 2000 and then the area percentage of agricultural land was dramatically decreased to 0.2 % of study area in the period of 2020.

5. Change in bare land: There was a little change in bare land between 2000 and 2020. The amount of bare land in Shwegyin River Basin was 145.1 km², accounting for 8.4% of the total area in 2000. In the period of 2020, the amount of bare land was fallen down and was 126.9 km² (7.3% of total area). Therefore, it was found that the amount of bare land in 2020 declined 1.1% of that in 2000.

6. CONCLUSION

GIS and remote sensing tools are powerful for assessing land use and land cover changes at watershed. Land use and land cover changes effect on wide range of consequences at all spatial and temporal scales. This paper aims investigating of land use and land cover changes detection occurred in Shwegyin River Basin before and after constructing dam between 2000 and 2020 using Landsat images. From studying of land use land cover change detection, it is found that the area percentage of water bodies was increased about 4% during the study period as well as after constructing the Shwegyin dam. Almost 80% of study area was covered by forest. The large amount of forest cover was existed before constructing Shwegyin dam and thus area amount was declined during one decade after finishing dam. In this study area, the area percentage of urban and built up land was gradually increased (3% and 7.9% respectively) in twenty years. Agricultural area was decreased and

bare land area was dropped down as a replacement of urbanized activities. It may be concluded that the land use and land cover change in Shwegyin River Basin has taken place significantly due to the construction of dam during the period 2000 to 2020. It is found that overall accuracy of 2020 is better than the period of 2000. Finally, the proper land use/cover management strategies need to protect these important land use/land cover and to obtain valuable information for better monitoring, mapping and understanding land-use/land cover changes over the time.

ACKNOWLEDGEMENT

First of all, the author would like to express the deepest gratitude to Dr Nyan Phone, Professor and Head of Civil Department, Technological University (Thanlyin) for his kind lead and true-line guidance for this study. The author would like to express her sincere gratitude to her supervisor Dr. Su Su Hlaing, Lecturer, Technological University (Thanlyin), for her valuable guidance and continuous support and for her patience and motivation. The author would like to express her thanks to her co-supervisor Daw Shwe War, Assistant Lecturer, Technological University (Thanlyin). Also, the author extends her thanks to U Ba Nyar Oo, Assistant Lecturer, Technological University (Thanlyin) for his supporting and his valuable guidance. Finally, the author would like to wish to acknowledge sincere gratitude to her father and mother for encouragement throughout the study.

REFERENCES

- [1] Lambin E.F., Geist H.J and Lepers E. "Dynamics of Land Use and Land Cover in Tropical Regions". Annual Review of Environment and Resources, Vol.28, no.1, pp. 205-210, 2003.
- [2] Li X., Zhao S., Yang H., Cong D., Zhang Z. "A Bi-Band Binary Mask Based Land-Use Change Detection Using Landsat 8 OLI Imagery". Sustainability, Vol. 9, no.3, pp.479-485, 2017.
- [3] Abd El-Kawy O.R., RØD J.K., Ismail H.A., Suliman A.S. "Land use and land cover change detection in the western Nile delta of Egypt using remote sensing data." Applied Geography, Vol.31, no.2, pp.483-488, 2011.
- [4] Jovanovic D., Govedarica M., Sabo F., Bugarinovic Z., Novovic O., Beker T. and Lauther M. "Land cover change detection by using remote sensing: A case study of Zlatibor (Serbia)". Vol.19 no.4, pp.162-166, 2015.
- [5] Mukhiddin Juliev, Alim Pulatov, Sven Fuchs and Johannes Hübl. "Analysis of Land Use Land Cover Change Detection of Bostanlik District, Uzbekistan" Pol. J. Environ. Stud. Vol. 28, No. 5, pp.3235-3242, 2019.
- [6] Mercy C Cheruto, Matheaus K Kauti, Patrick D Kisangau and Patrick Kariuki. "Assessment of Land Use and Land Cover Change Using GIS and Remote Sensing Techniques: A Case Study of Makuani County, Kenya" Cheruto et al., J Remote Sensing & GIS, Vol.5, Issue.4, November, 03, 2016.
- [7] Amare Sewnet, "Land use/cover change at Infray watershed by using GIS and remote sensing techniques, northwestern Ethiopia". Intl. J. River Basin Management, Vol. 14, No. 2, pp. 133-142, June 2016.

[8] S. Poongothai, N. Sridhar, R. Arun Shourie. “*Change Detection of Land use/ Land Cover of a Watershed using Remote Sensing and GIS*”. International Journal of Engineering and Advanced Technology (IJEAT) ISSN: 2249-8958, Vol.3 Issue.6, August 2014.

[9] William S. Ruto, “*Land Use-Land-Cover Changes in Saiwa Swamp Watershed, Western Kenya.*” International Journal of Research in Environmental Science Vol. 4, Issue .4, PP 1-7, 2018.

[10] Mukhiddin Juliev, “*Analysis of Land Use Land Cover Change Detection of Bostanlik District, Uzbekistan*”. Pol. J. Environ. Stud. Vol. 28, No. 5, pp.3235-3242, 2019.

[11] Gebrekidan Worku, Habtamu Temesgen and Amare Bantider. “*Land use and land cover change in Ameleke Watershed, South Ethiopia*”. Journal of Natural Sciences Research Vol.4, No.14, pp.42-47, 2014.

[12] Amare Sewnet. “*Land Use/Cover Change at Infraz Watershed by using GIS and Remote Sensing Technique, Northern Ethiopia*”. Journal of Landscape Ecology, Vol. 8, No. 2, pp.133-142, June 2016.